中國科學院物理研究所
Institute of Physics, Chinese Academy of Sciences

量子模拟多体物理

Heng Fan（范桁）
Institute of Physics
Chinese Academy of Sciences

2020年5月14日

Outline

1. 量子计算模拟多体物理主要进展
2. 量子计算优势（经典难）体现在什么地方？
3. 量子计算模拟多体物理适用于哪些问题?
4. 量子计算模拟怎样超越经典计算（量子优势）？
5. 量子计算实用化展望

1 量子计算模拟

量子模拟

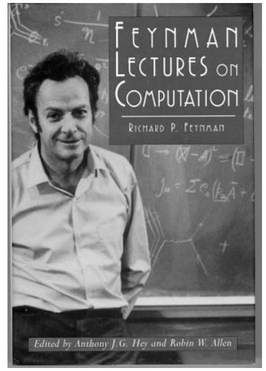

量子计算机可有效模拟物理过程

"Nature isn't classical, dammit, and if you want to make a simulation of Nature, you'd better make it quantum mechanical, and by golly it's a wonderful problem because it doesn't look so easy."

R. P. Feynman, 1981

Simulating Physics with Computers

Richard P. Feynman

Department of Physics, California Institute of Technology, Pasadena, California 91107

Received May 7, 1981

two parts.

4. QUANTUM COMPUTERS—UNIVERSAL QUANTUM SIMULATORS

The first branch, one you might call a side-remark, is, Can you do it with a new kind of computer—a quantum computer? (I'll come back to the other branch in a moment.) Now it turns out, as far as I can tell, that you can simulate this with a quantum system, with quantum computer elements.

Int.J.Theor.Phys. 1982

1 数字式量子模拟（digital simulation）

物理基础	量子计算机实现

$$i\hbar\frac{d}{dt}|\phi\rangle = H|\varphi\rangle$$ 薛定谔方程

$$|\varphi(t)\rangle = \exp\{-i\hbar Ht\}|\varphi(0)\rangle.$$

$$U = \exp\{-i\hbar Ht\}$$

$$U = (\exp\{-i\hbar H\Delta t\})^{t/\Delta t}$$

$$H = \sum_{l=1}^{M} H_l.$$

$$U(\Delta t) = e^{-i\hbar\sum_l H_l \Delta t} = \prod_l e^{-i\hbar H_l \Delta t} + \mathcal{O}((\Delta t)^2).$$

$$U(\Delta t) \approx \prod_l \exp\{-i\hbar H_l \Delta t\}.$$

Trotter-Suzuki分解

$|\varphi(0)\rangle$

初态

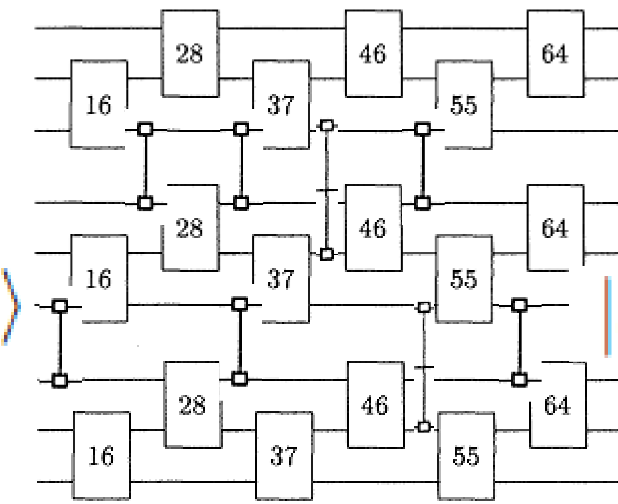

$|\varphi(t)\rangle$

末态

$U(\Delta t)$ $U(\Delta t)$ $U(\Delta t)$ $U(\Delta t)$

时间演化

1 数字式量子模拟动力学相变: 分解为量子逻辑门操作

横场Ising模型

$$H(g) = -\sum_{j}^{L} \sigma_j^z \sigma_{j+1}^z + g\sigma_j^x.$$

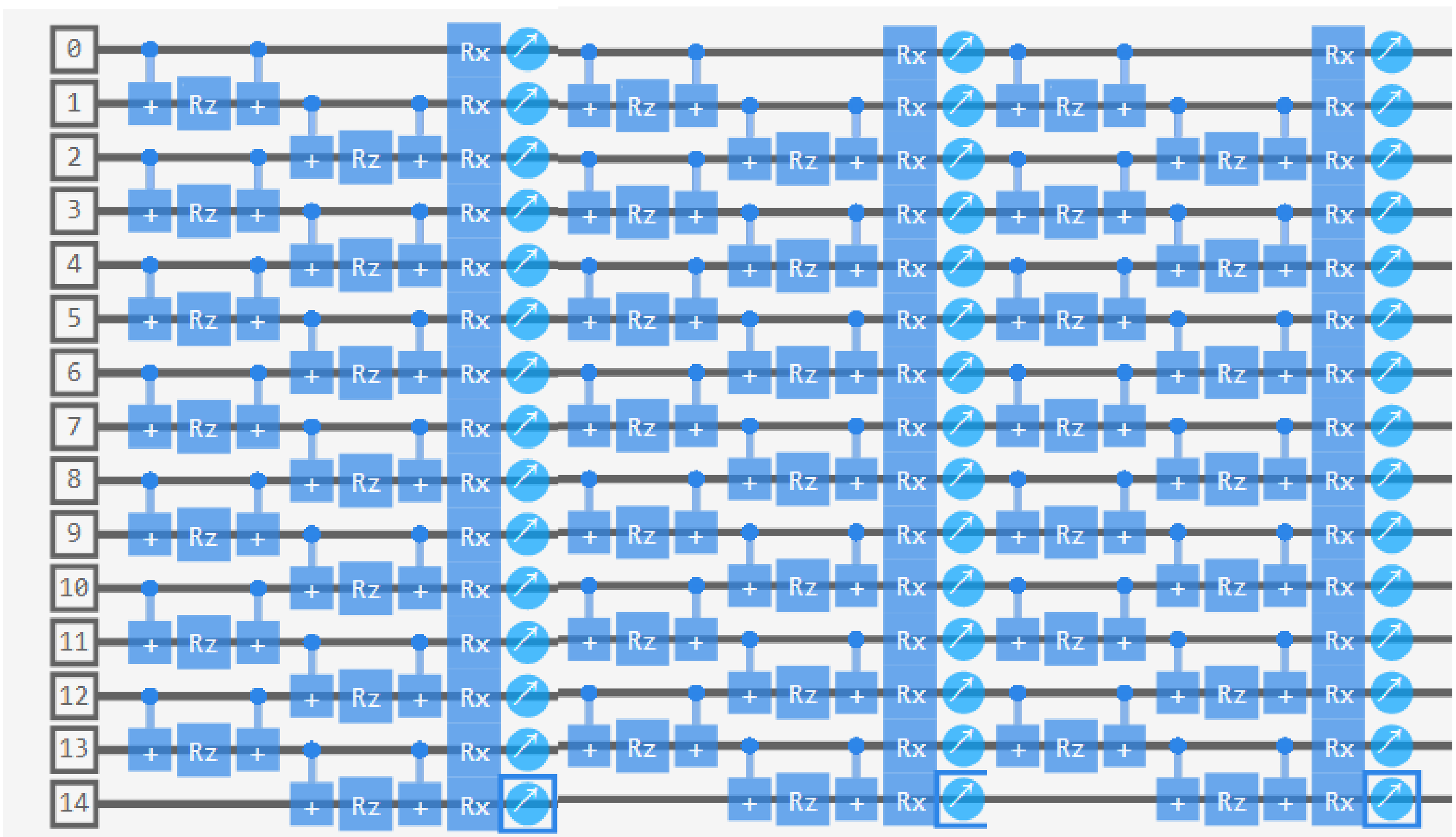

时间演化

一个例子：量子模拟动力学相变

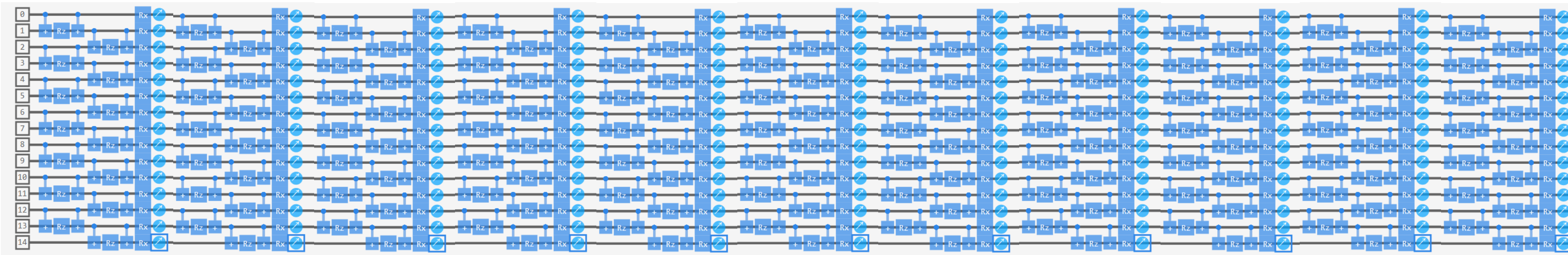

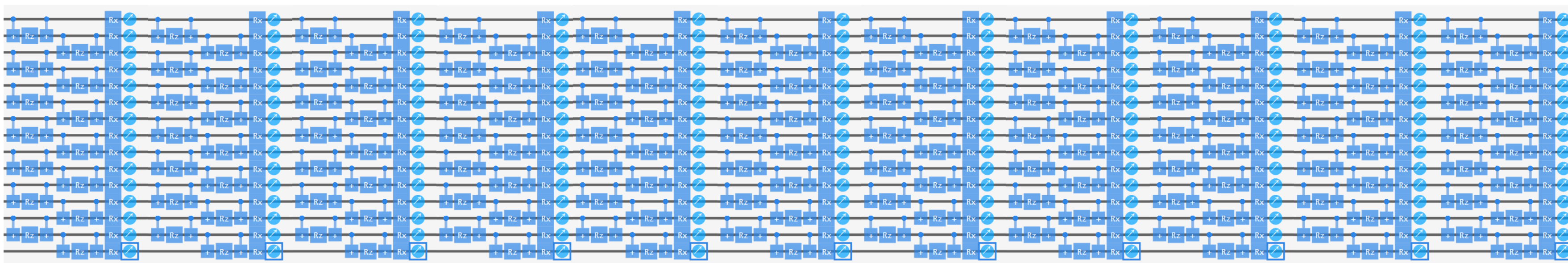

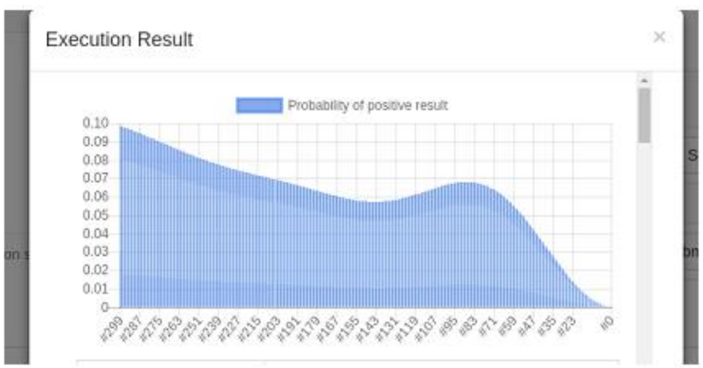

Figure 4: L = 28, $g_1 = 0.5$

时间演化

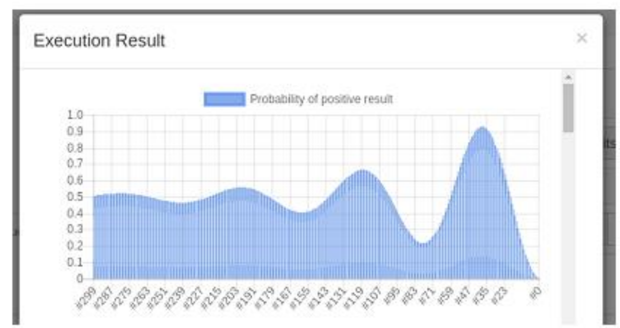

Figure 5: L = 28, $g_1 = 4$

时间演化

一个例子：量子模拟动力学相变

g=0->4，通过相变点
有动力学相变点（QtVM）

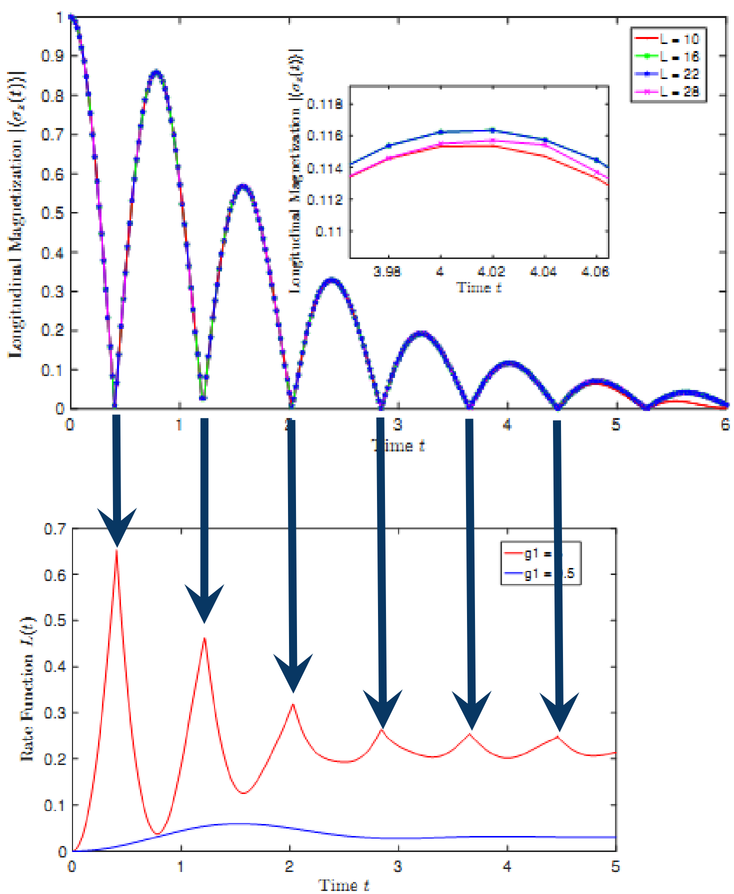

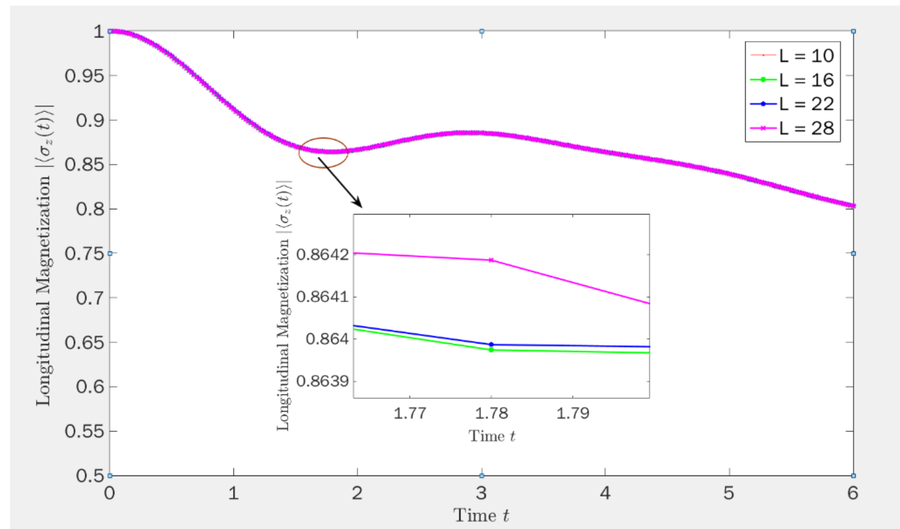

g=0->0.5，没通过相变点
没有动力学相变点

理论解析结果：
Loschmidt amplitude for dynamical phase transition

1 量子模拟动力学相变：与精确对角化的对比

g=2，通过相变点：12个量子比特

精确对角化与QtVM结果相同

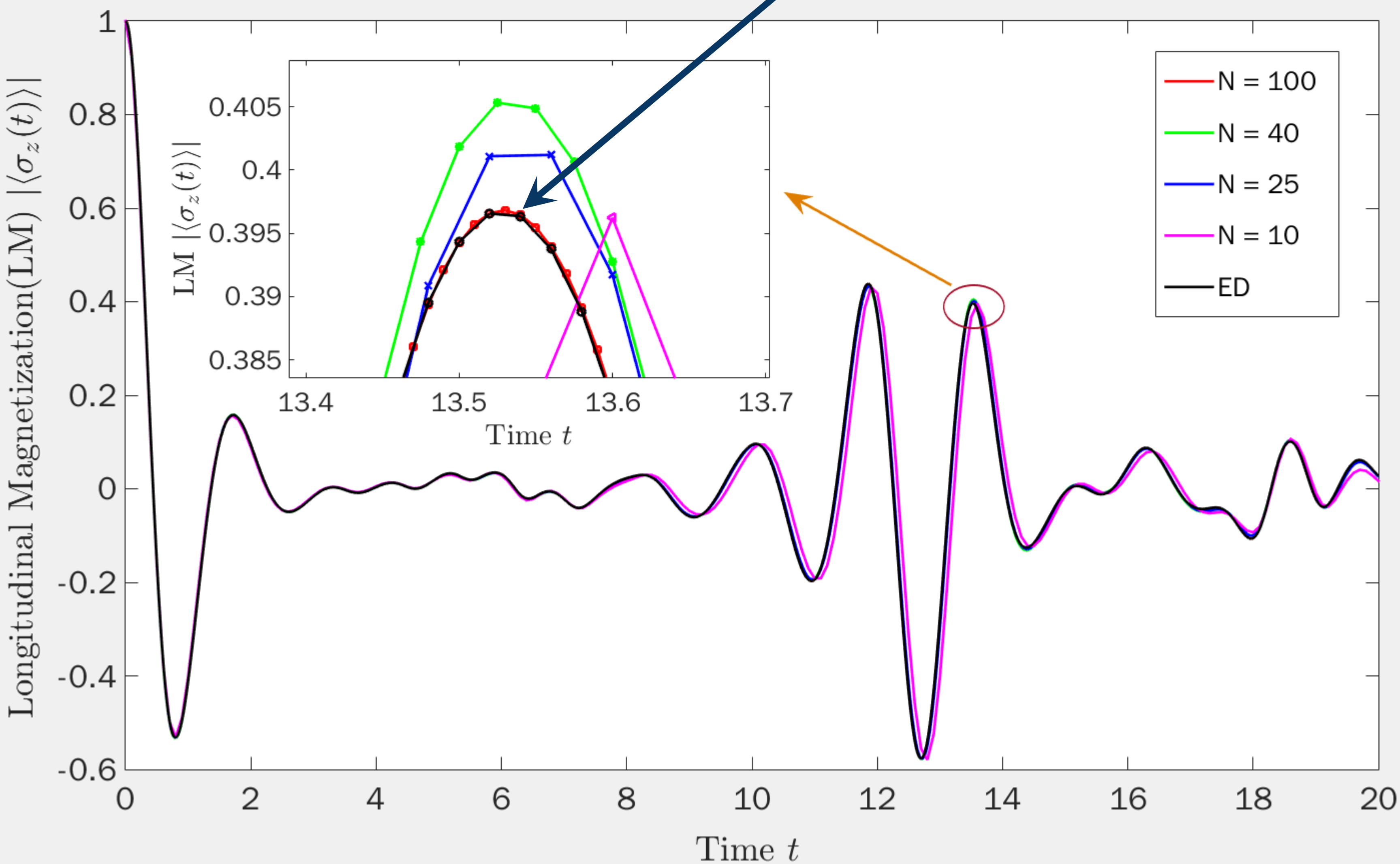

Analog Quantum Simulator

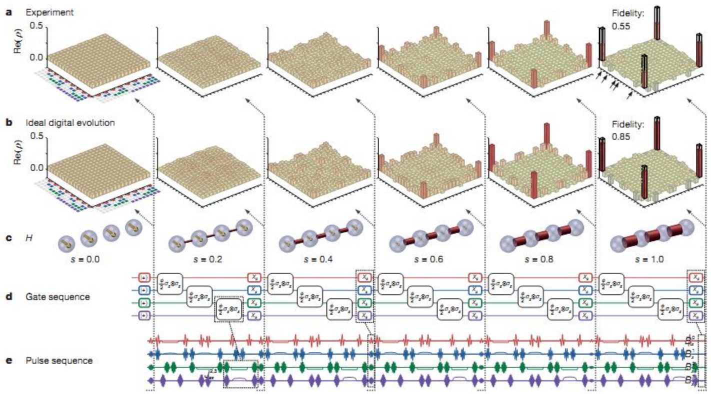

Martinis group, Nature 2016.

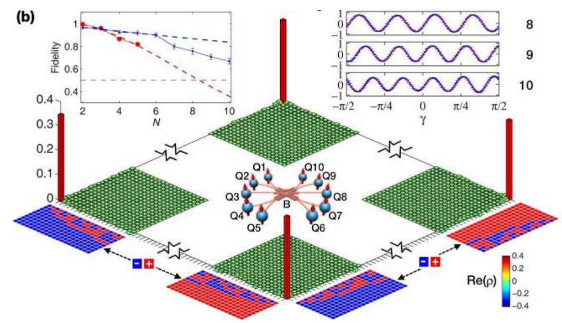

10-qubit GHZ
PRL119， 2017.

Time dependent wave function can be readout by state tomography, physical quantities can then be obtained

$$H_{\rm I} = -B_{x,1}\sum_i \sigma_x^i$$

$$H_{\rm P} = -\sum_i \left(B_z^i\sigma_z^i + B_x^i\sigma_x^i\right) - \sum_i \left(J_{zz}^{i,i+1}\sigma_z^i\sigma_z^{i+1} + J_{xx}^{i,i+1}\sigma_x^i\sigma_x^{i+1}\right)$$

$$\mathcal{H} = \sum_{i=1}^{9} \delta_i \hat{n}_i + \frac{\eta_i}{2}\hat{n}_i(\hat{n}_i - 1) + \sum_{i=1}^{8} g_i\left(\hat{a}_i^\dagger \hat{a}_{i+1} + \hat{a}_i \hat{a}_{i+1}^\dagger\right)$$

$$\frac{H}{\hbar} = \sum_{i<j} J_{ij}(\sigma_i^+\sigma_j^- + \sigma_i^-\sigma_j^+) + \sum_i (h_i + \delta h_i)\sigma_i^+\sigma_i^-,$$

Programmable control

量子模拟进展：Analog Simulation

Special purpose, analog simulation

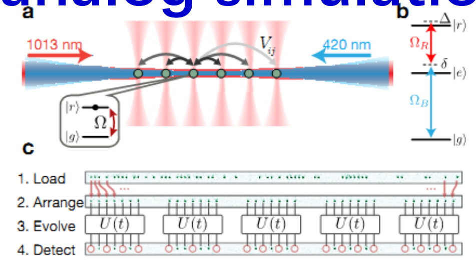

51 atom: Lukin group, Nature 551, 579(17)

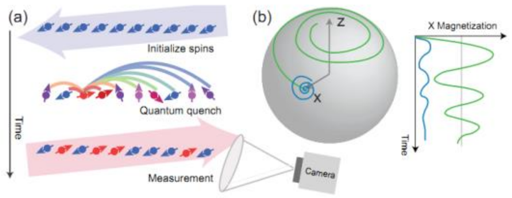

53 qubits: Monroe group, Nature 551, 601 (17)

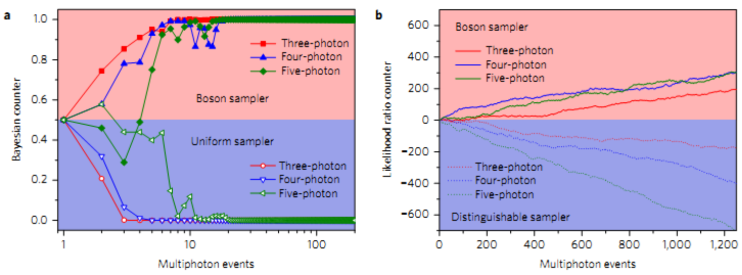

photon：5-10 qubits: Pan group,
Nature Photon. (2017); PRL 117, 210502 (2016).

Universal

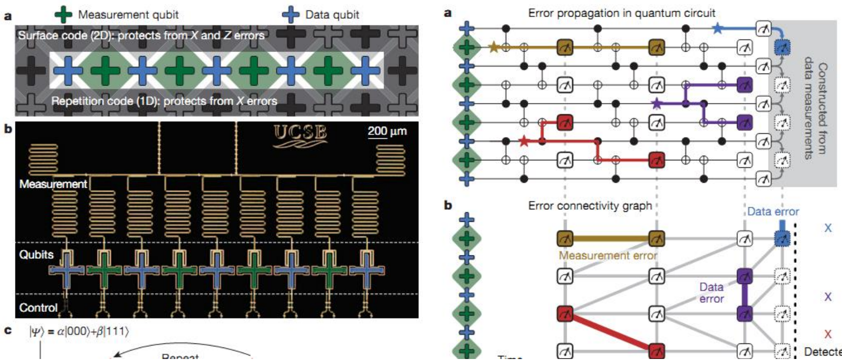

9 qubits: Martinis group, Nature (2015)

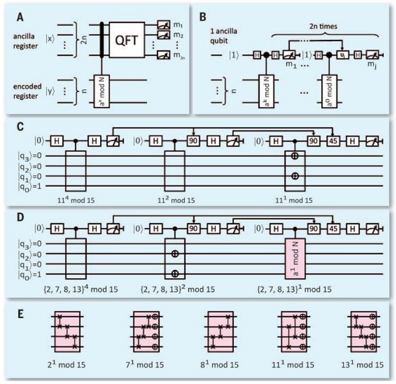

5 qubits: Blatt group, Science (2015)

Scalability

Quantum Simulator： Rydberg atoms, Ising型

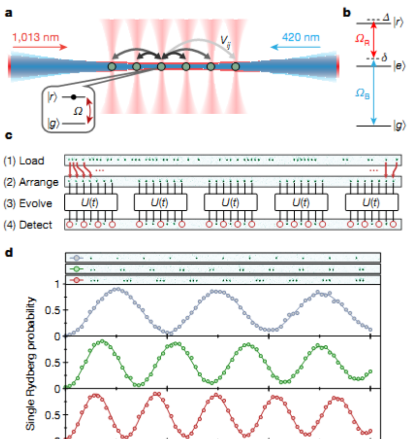

$$\frac{\mathcal{H}}{\hbar}=\sum_i \frac{\Omega_i}{2}\sigma_x^i-\sum_i \Delta_i n_i+\sum_{i<j} V_{ij} n_i n_j$$

$$V_{ij}=C/R_{ij}^6$$

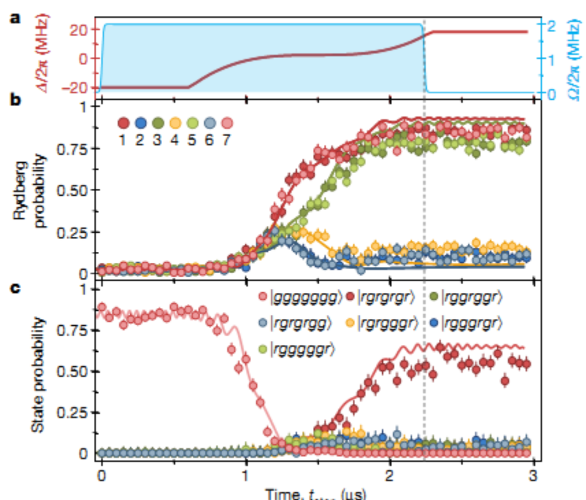

51 atom: Lukin group, Nature 551, 579(17)

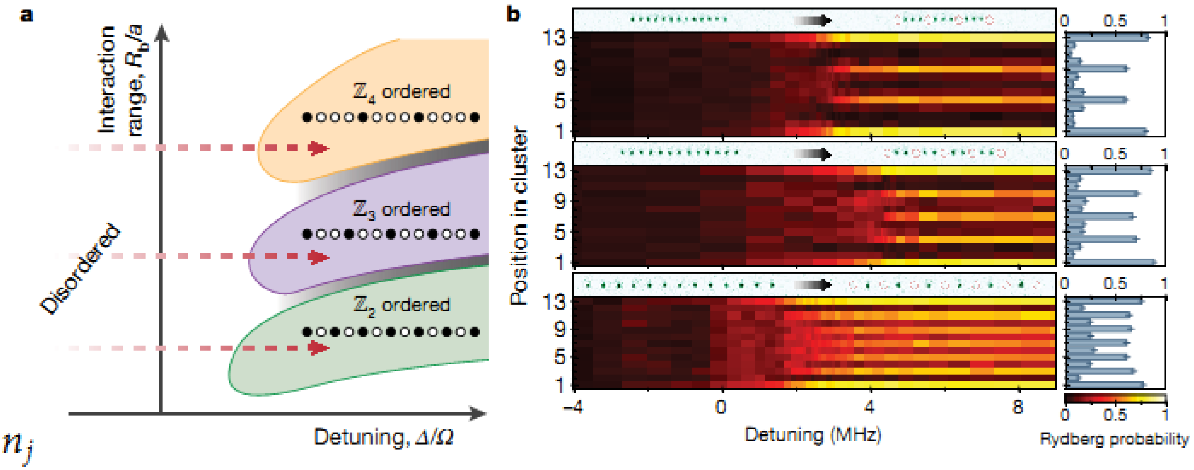

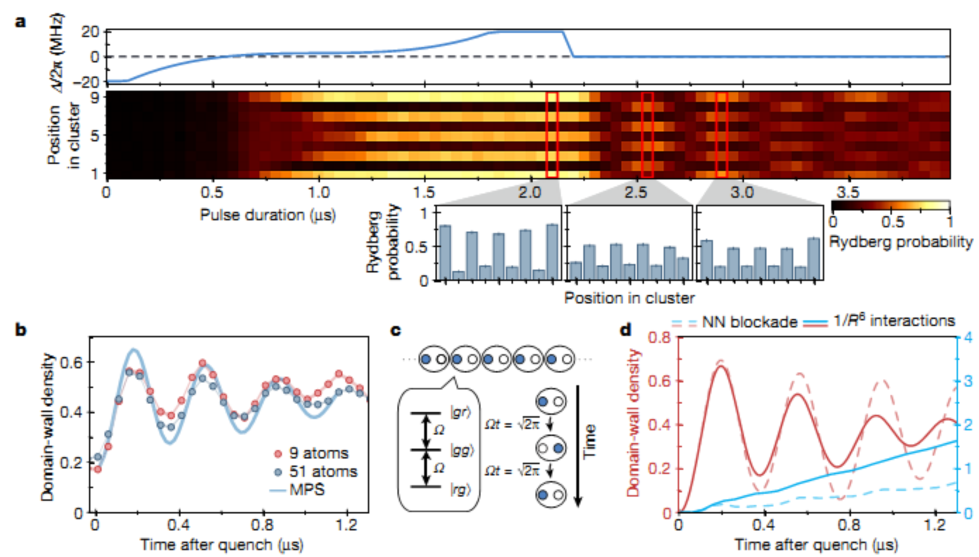

Trapped ions quantum simulator：横场Ising型

53 qubits: Monroe group, Nature 551, 601 (17)

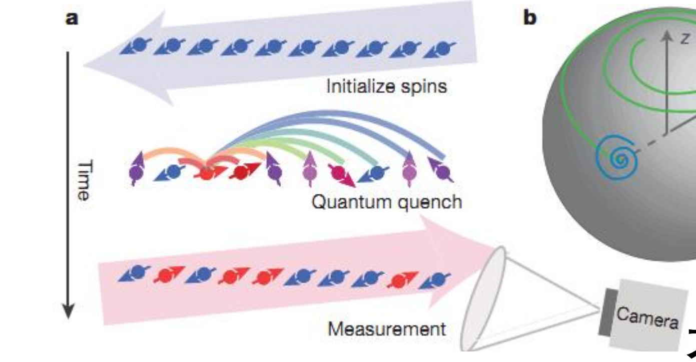

模型

$$H = \sum_{i<j} J_{ij}\sigma_i^x\sigma_j^x + B_z\sum_i \sigma_i^z$$

$$J_{ij} \approx J_0/|i-j|^\alpha$$

不同场强下的动力学不同

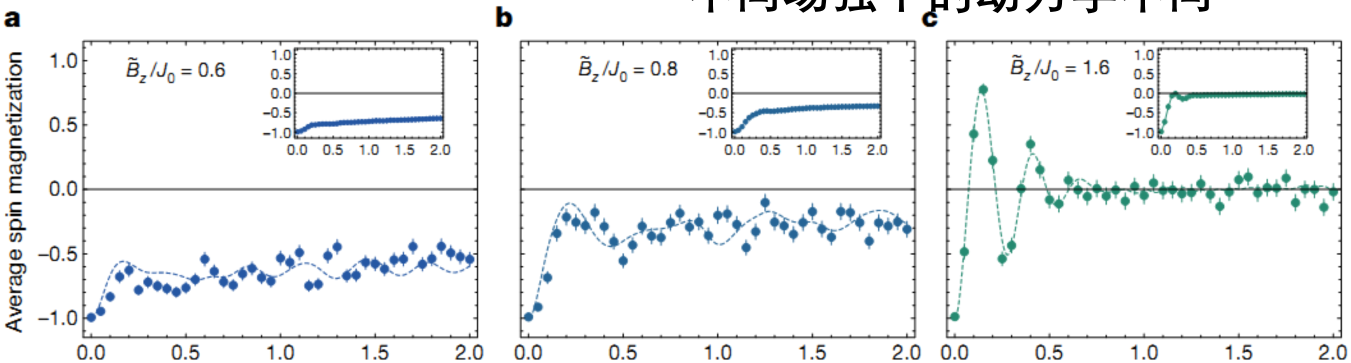

测量量

$$\langle \sigma^x(t)\rangle = \frac{1}{N}\sum_i \langle \sigma_i^x(t)\rangle$$

$$C_2 = \frac{1}{N^2}\sum_{i,j}\langle \sigma_i^x\sigma_j^x\rangle$$

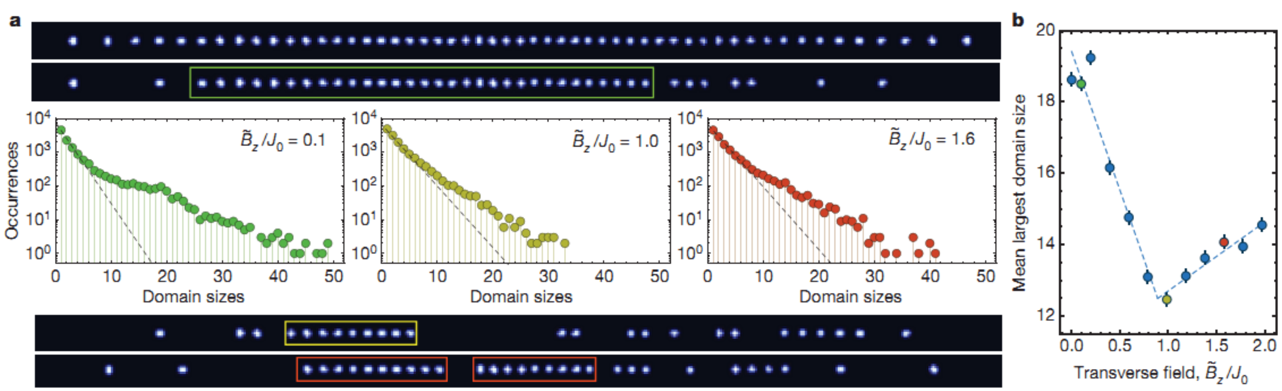

Time-crystal: trapped ions and NV (含时调控)

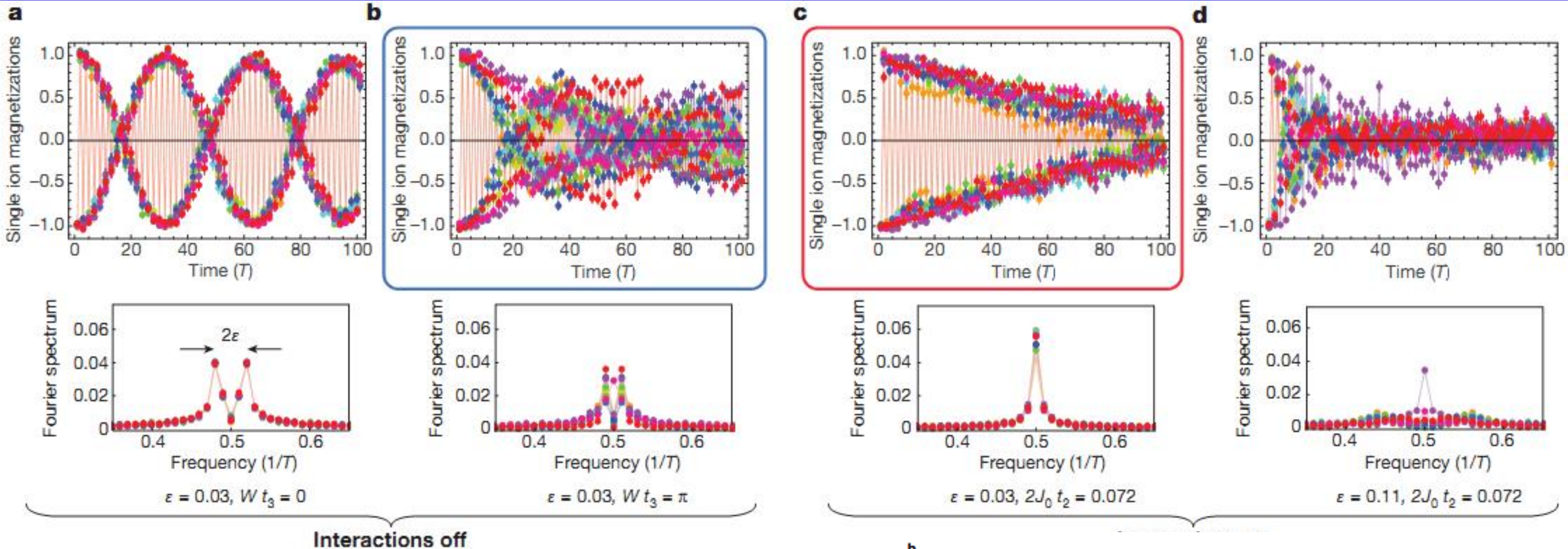

$$H = \begin{cases} H_1 = g(1-\varepsilon)\sum_i \sigma_i^y & \text{time } t_1 \\ H_2 = \sum_i J_{ij}\sigma_i^x\sigma_j^x & \text{time } t_2 \\ H_3 = \sum_i D_i\sigma_i^x & \text{time } t_3 \end{cases}$$

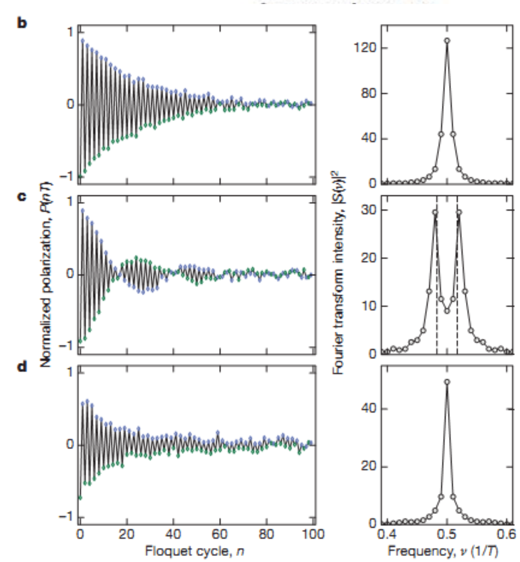

Nature 543, 217 (2017)

Nature 543, 221 (2017)

量子机器学习

$$\mathcal{U}_{\Phi(x)} \doteq U_{\Phi(x)} H^{\otimes n} U_{\Phi(x)} H^{\otimes n}$$

$$U_{\Phi(x)} = \exp\left(i \sum_{S\subseteq[n]} \phi_S(x) \prod_{i\in S} Z_i \right)$$

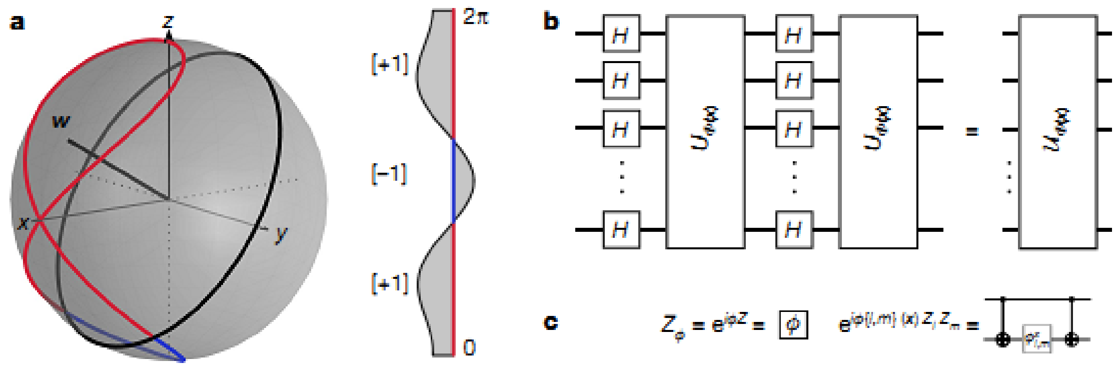

实验实现线路

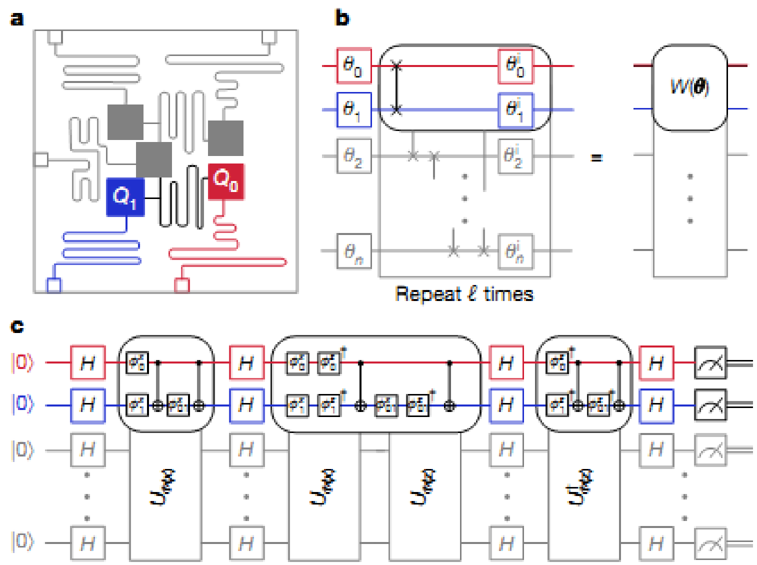

Fig. 2 | Experimental implementations. a, Schematic of the

Nature 567, 209 (2019)

Supervised learning with quantum-enhanced feature spaces

Many-body localization

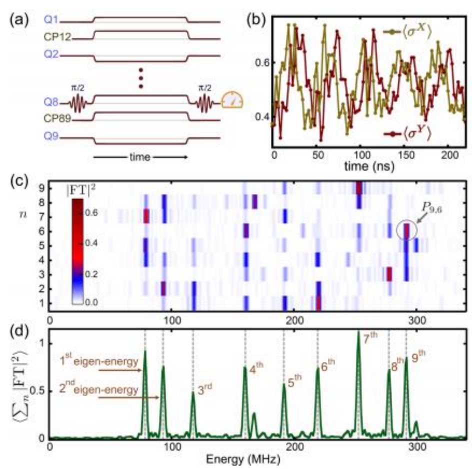

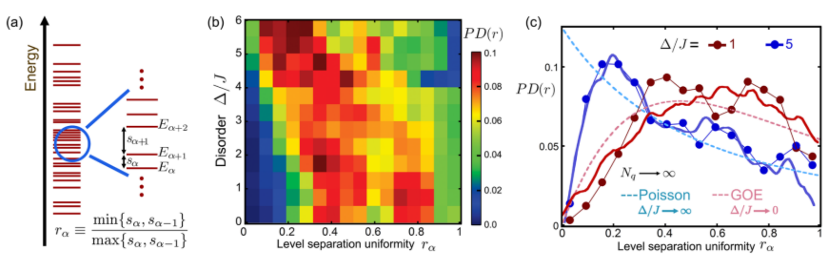

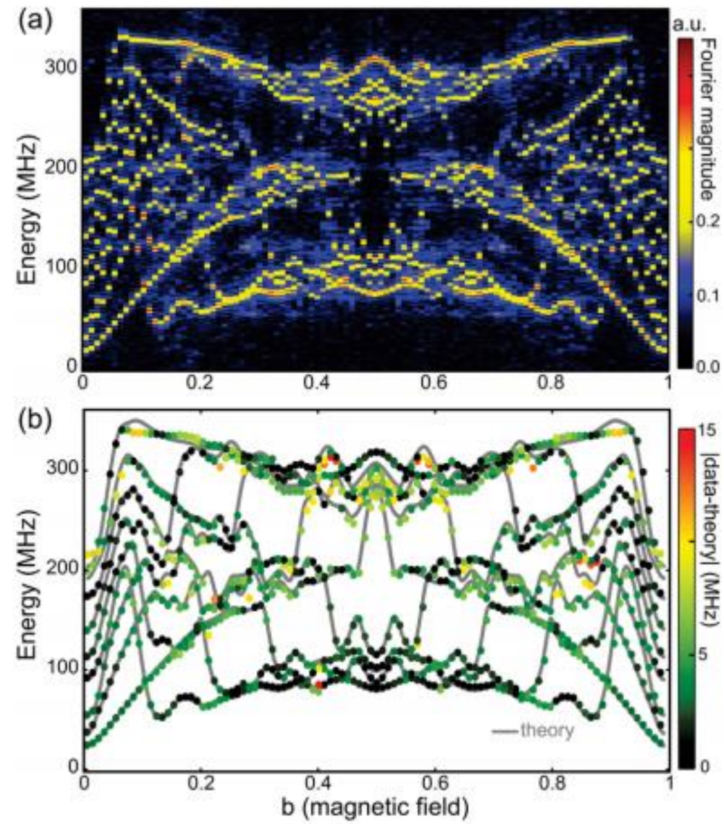

$$H_{BH} = \sum_{n=1}^{9} \mu_n a_n^\dagger a_n + \frac{U}{2}\sum_{n=1}^{9} a_n^\dagger a_n (a_n^\dagger a_n - 1) + J\sum_{n=1}^{8} a_{n+1}^\dagger a_n + a_n^\dagger a_{n+1},$$

$$|\psi(t)\rangle = \sum_\alpha C_\alpha e^{-iE_\alpha t/\hbar}|\phi_\alpha\rangle$$

能谱读出

- **Google Martinis group, Science ‘17.**

Many-body localization

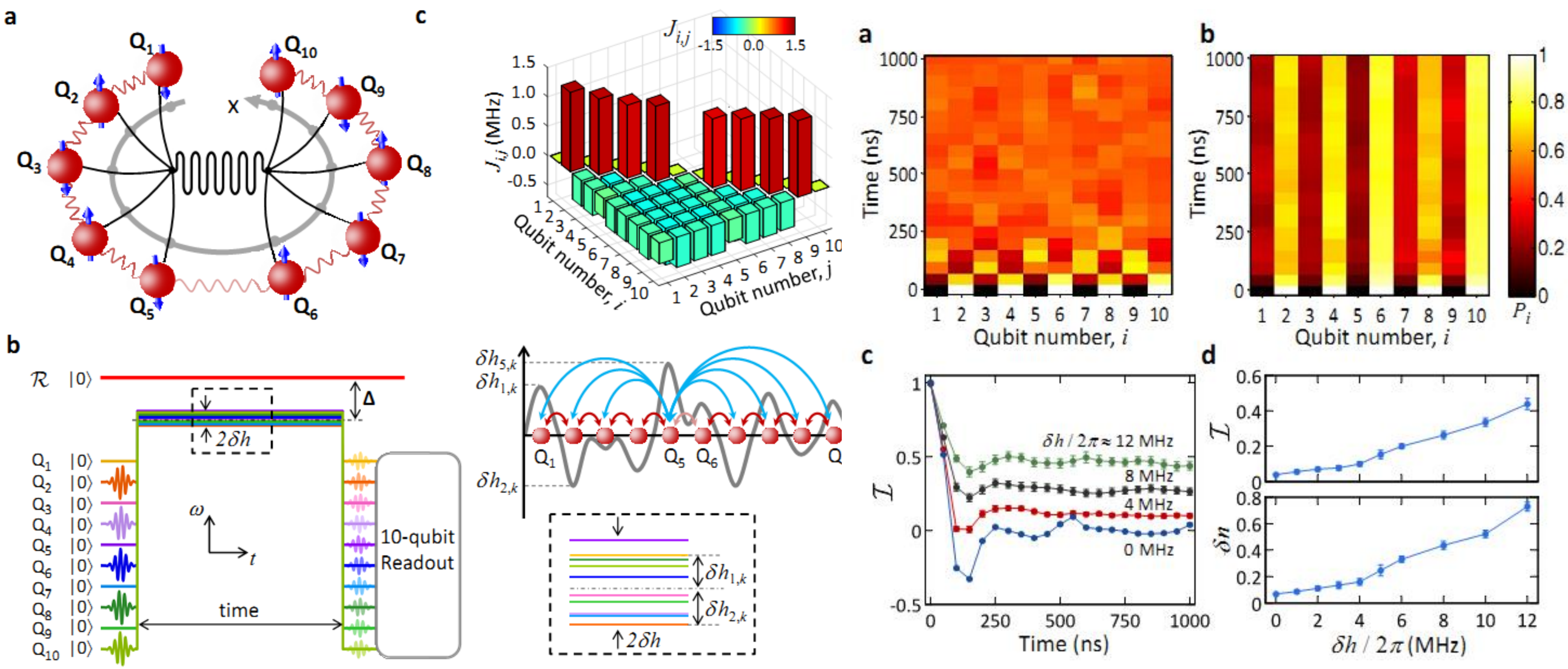

- **Many-body localization with a 10 qubits quantum processor，PRL 120, 050507 (2018).**

Many-body localization

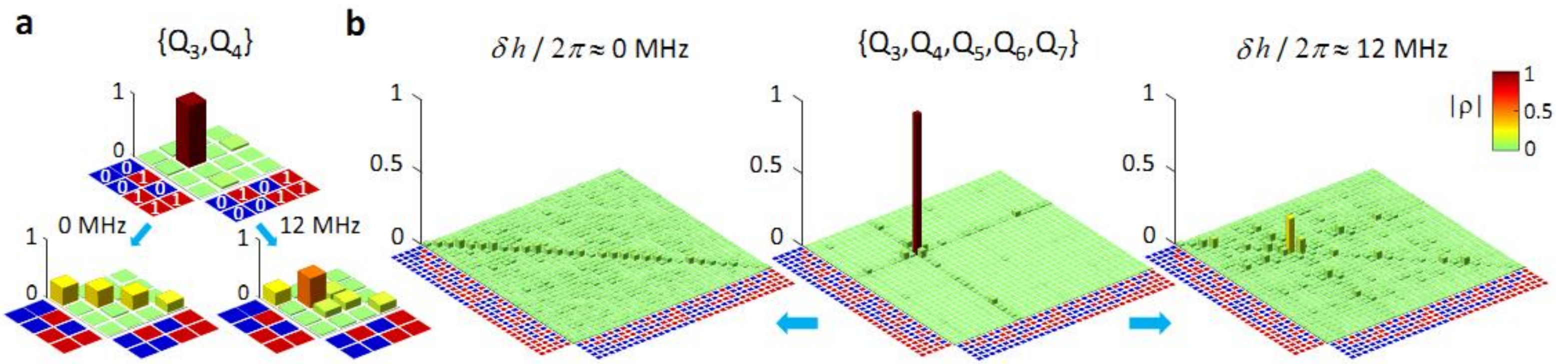

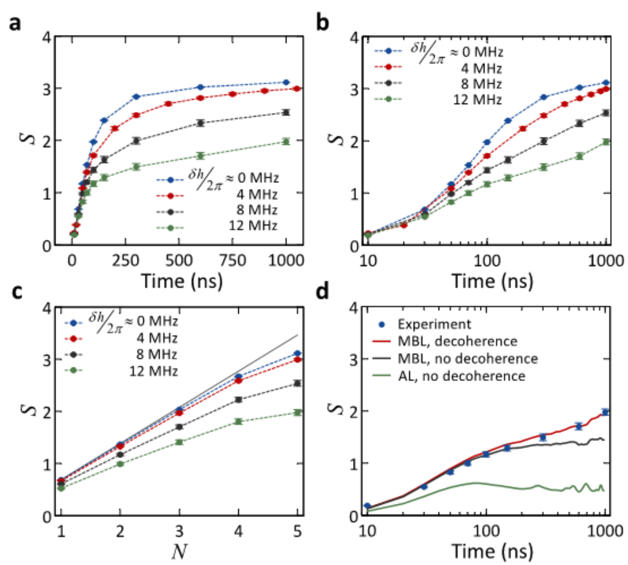

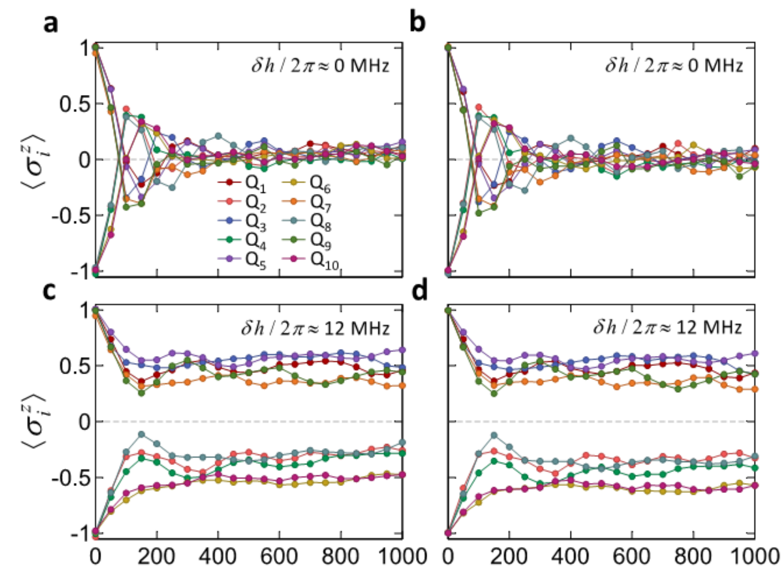

Phys. Rev. Lett. 120, 050507 (2018).

$$\frac{H}{\hbar} = \sum_{i<j} J_{ij}(\sigma_i^+\sigma_j^- + \sigma_i^-\sigma_j^+) + \sum_i (h_i + \delta h_i)\sigma_i^+\sigma_i^-$$

Kai Xu,[1] Jin-Jun Chen,[2,3] Yu Zeng,[2,3] Yu-Ran Zhang,[2,3] Chao Song,[1] Wuxin Liu,[1] Qiujiang Guo,[1] Pengfei Zhang,[1] Da Xu,[1] Hui Deng,[2] Keqiang Huang,[2,3] H. Wang,[1,4,*] Xiaobo Zhu,[4,†] Dongning Zheng,[2,3] and Heng Fan[2,3,‡]

Many-body localization：不同平台测量不同观测量

$$H_{\mathrm{XY}} = \hbar \sum_{i<j} J_{ij}(\sigma_i^+ \sigma_j^- + \sigma_i^- \sigma_j^+) + \hbar B \sum_j \sigma_j^z$$

$$H_{\mathrm{D}} = \hbar \sum\nolimits_j \Delta_j \sigma_j^z \text{ and } \Delta_j \text{ the magnitude of disorder}$$

$$\hat{\mathcal{H}} = -J\sum_i (\hat{a}_i^\dagger \hat{a}_{i+1} + h.c.) + \frac{U}{2}\sum_i \hat{n}_i(\hat{n}_i - 1) + W\sum_i h_i \hat{n}_i$$

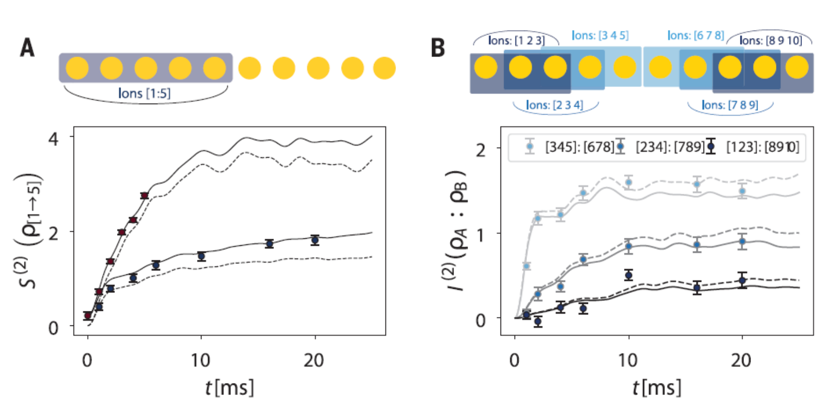

Fig. 4. Spread of quantum correlations under H_{XY} with and without disorder. The Hamiltonian

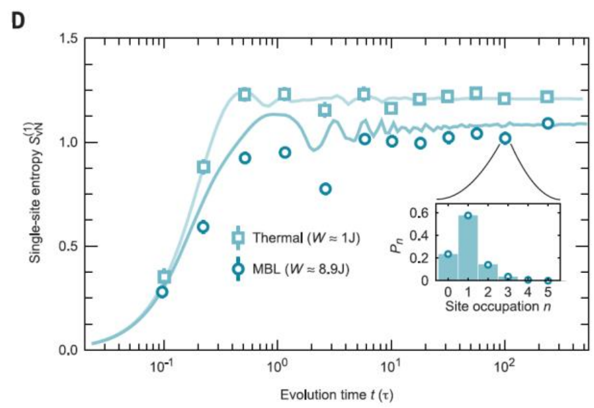

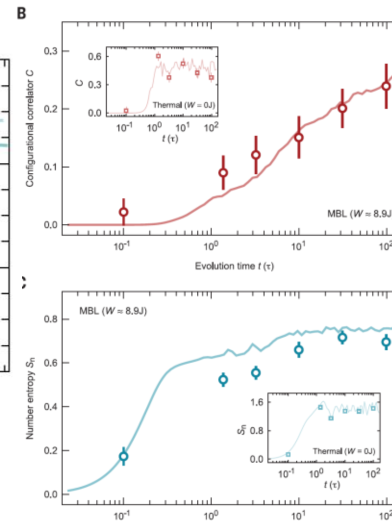

离子阱系统：热化/局域化，参数 Δ_j

冷原子光晶格：热化/局域化，参数W

1. Probing entanglement in a many-body–localized system, A. Lukin et al., Science 364, 256 (2019).

2. Probing Rényi entanglement entropy via randomized measurements, Tiff Brydges…P. Zoller, R. Blatt, C. F. Roos, Science 364, 260 (2019).

4 有噪音中等规模量子计算与量子模拟

利用19个超导量子比特模拟不同系统能量mobility edge现象

系统能量和无序强度所对应的热化和局域化相图

未解决问题：当系统很大时是否还是一个弓形结构

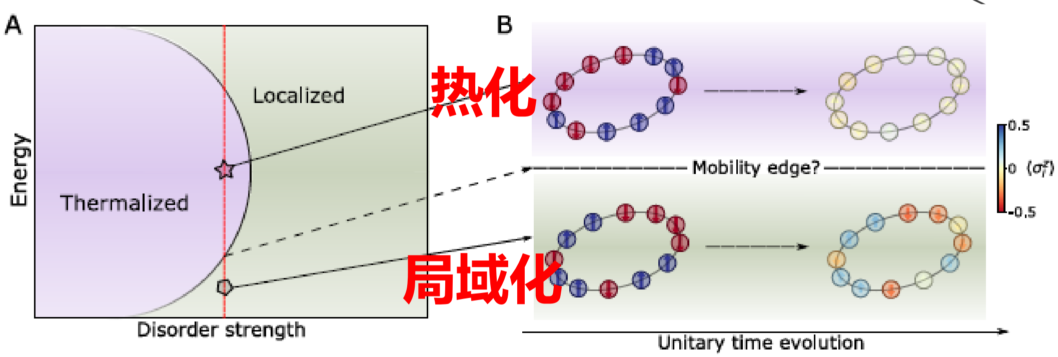

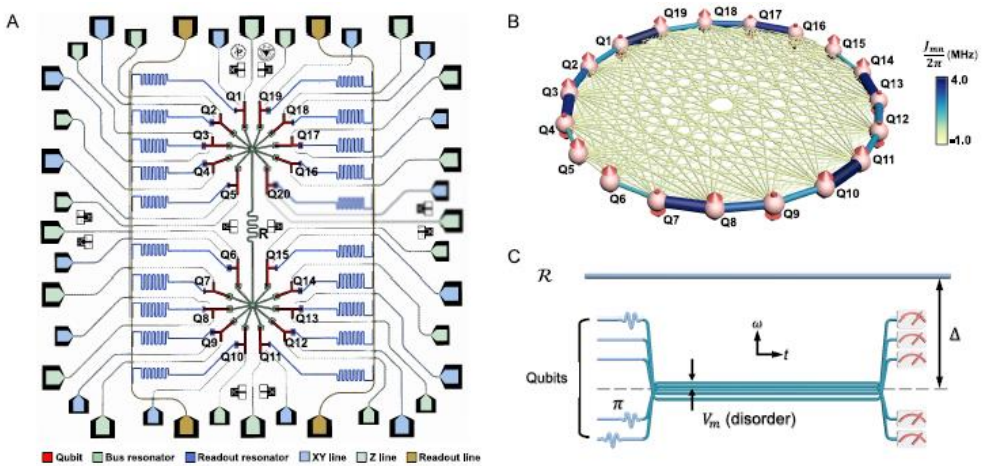

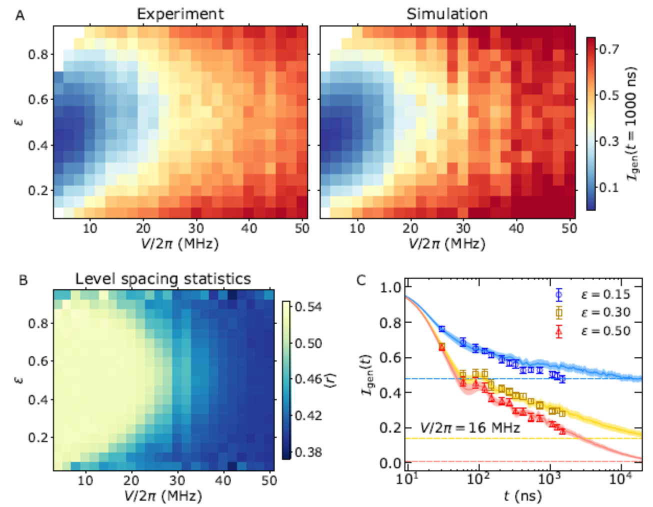

Q. Guo et al., arXiv:1912.02818.

5 Device with 24 qubits in a ladder configuration

Simulation of Bose-Hubbard ladder model

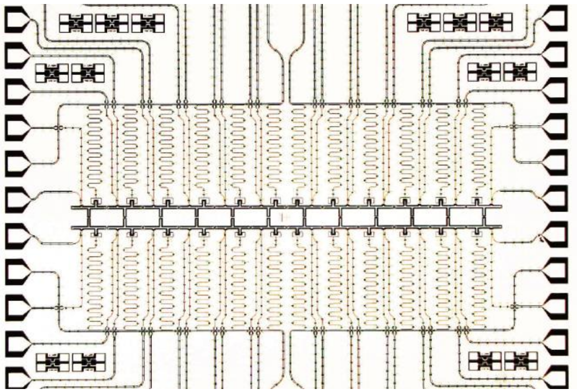

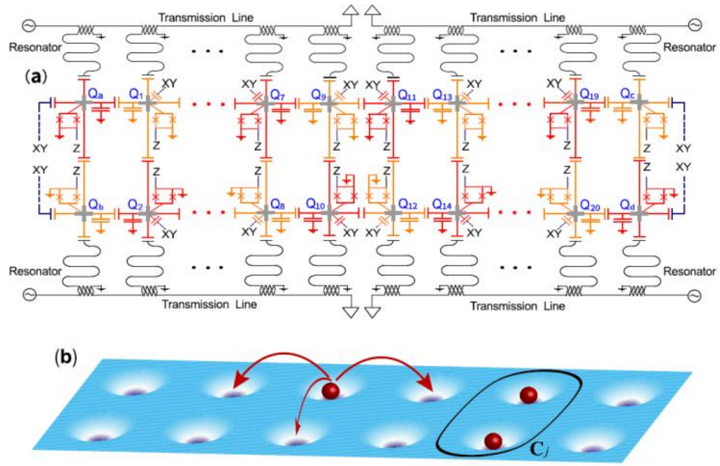

$$H = \sum_{j\nu} J_{j\nu}(\hat{a}^{\dagger}_{j\nu}\hat{a}_{(j+1)\nu} + \mathrm{H.c.}) + \sum_{j} J_{jR}(\hat{a}^{\dagger}_{jA}\hat{a}_{jB} + \mathrm{H.c.})$$

$$+ \frac{U}{2}\sum_{j\nu}\hat{n}_{j\nu}(\hat{n}_{j\nu} - 1) + \sum_{j\nu} h_{j\nu}\hat{n}_{j\nu}, \qquad (1)$$

Phys. Rev. Lett. 123, 050502 (2019)

5 Device with 24 qubits in a ladder configuration

Simulation of Bose-Hubbard ladder model

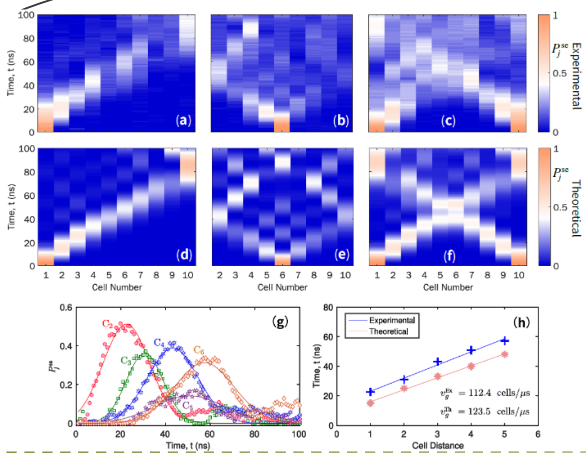

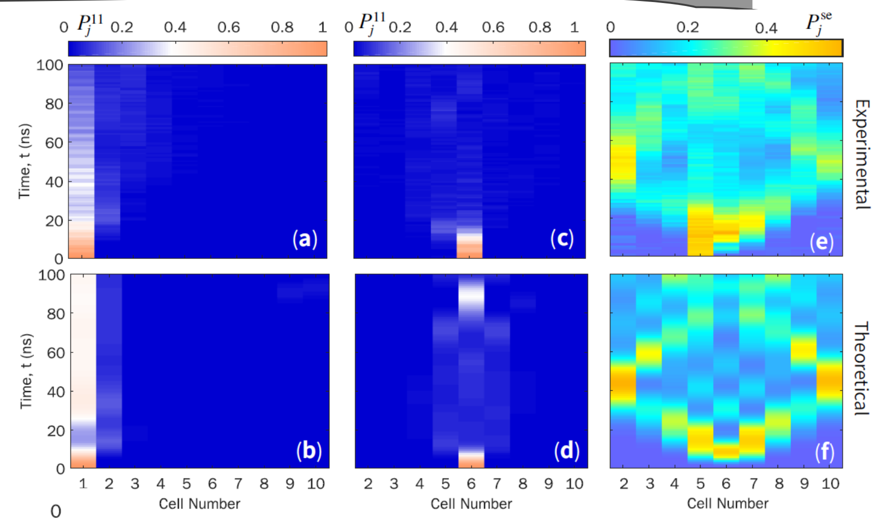

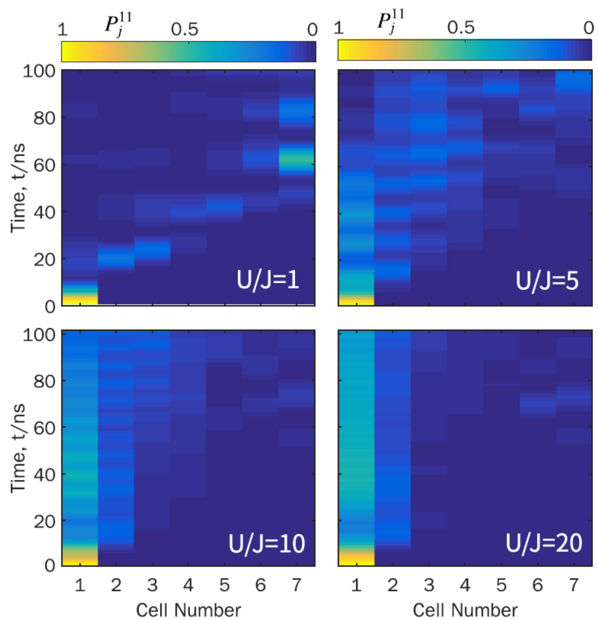

Localized state at a boundary

due to large on-site interactions

Phys. Rev. Lett. 123, 050502 (2019)

4 有噪音中等规模量子计算与量子模拟

利用16个超导量子比特模拟LMG模型的动力学相变

模型： $H_1/\hbar = \sum_{i\neq j}^{N} \lambda_{ij}(\sigma_i^+\sigma_j^- + \sigma_i^-\sigma_j^+) + h^x \sum_{j=1}^{N} \sigma_j^x$ → $H_{\mathrm{LMG}} = (J/N)(S^z)^2 + \mu S^x$

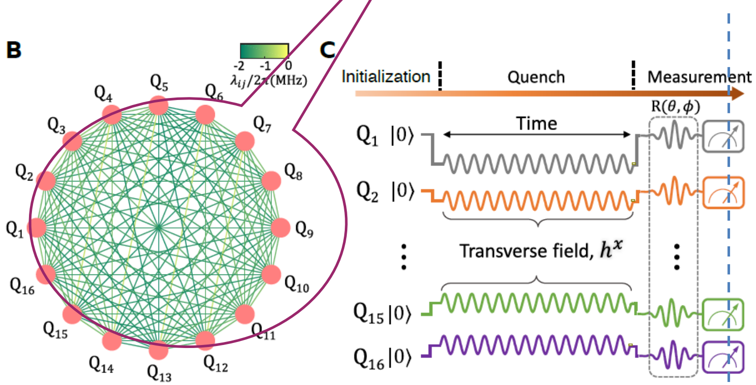

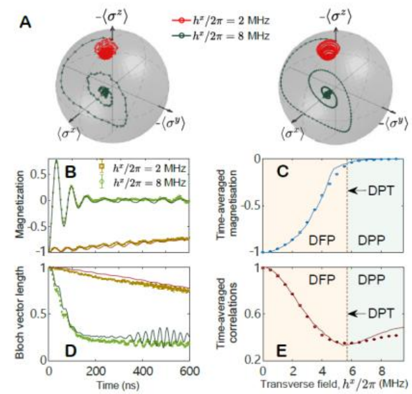

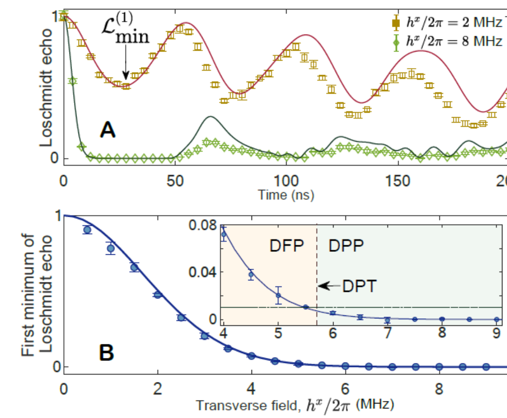

系统在不同横场强度下的动力学演化过程

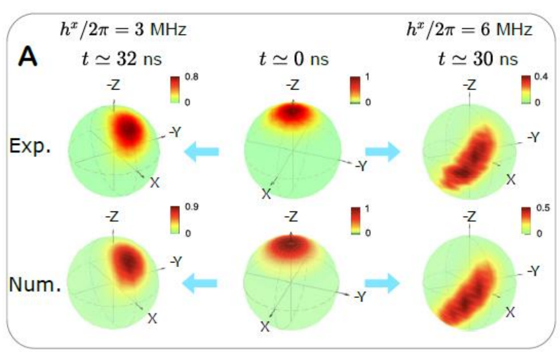

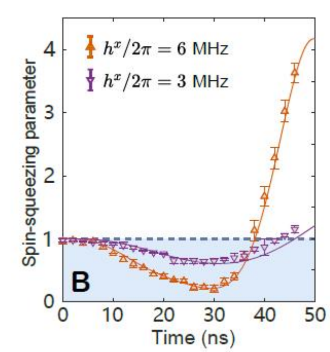

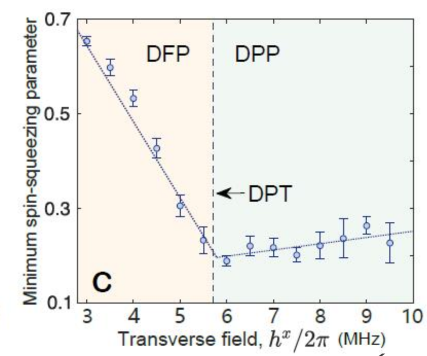

K. Xu et al., arXiv:1912.05150.

4 利用时间演化模拟物理问题

超导量子模拟莫特绝缘体性质

$$\mathcal{H}_{\mathrm{BH}}/\hbar = -\sum_{\langle ij\rangle} J_{ij} a_i^{\dagger} a_j + \frac{U}{2}\sum_i n_i(n_i-1) + \sum_i \epsilon_i n_i$$

RESEARCH ARTICLE

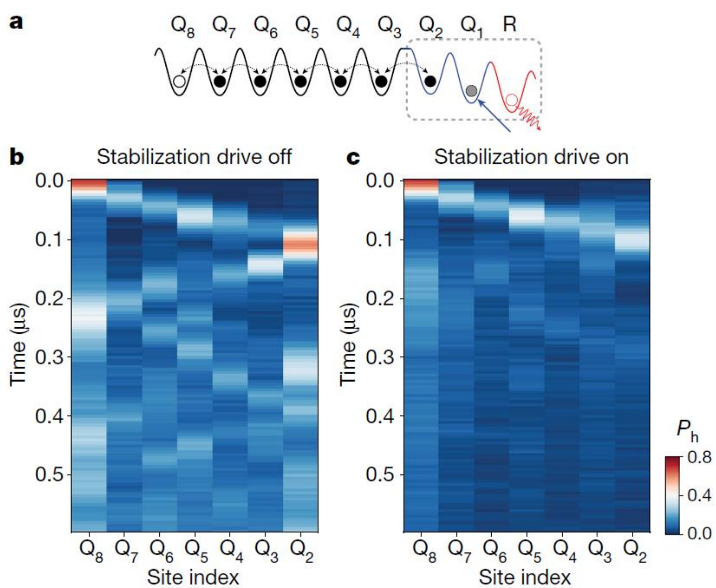

Fig. 5 | Dynamics of a hole defect in the Mott insulator. a, To explore

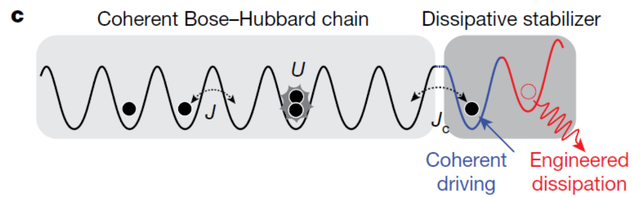

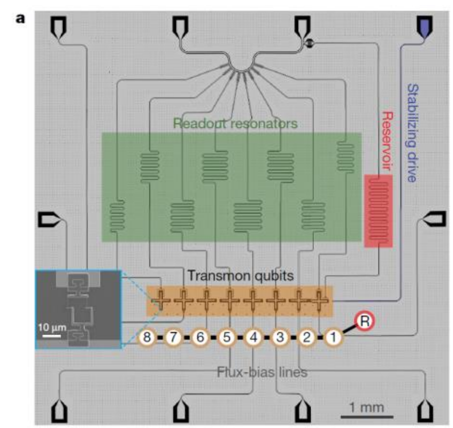

A dissipatively stabilized Mott insulator of photons, Ruichao Ma… David I. Schuster, Nature 566, 51 (2019).

Background： quantum walks(归入量子态演化)

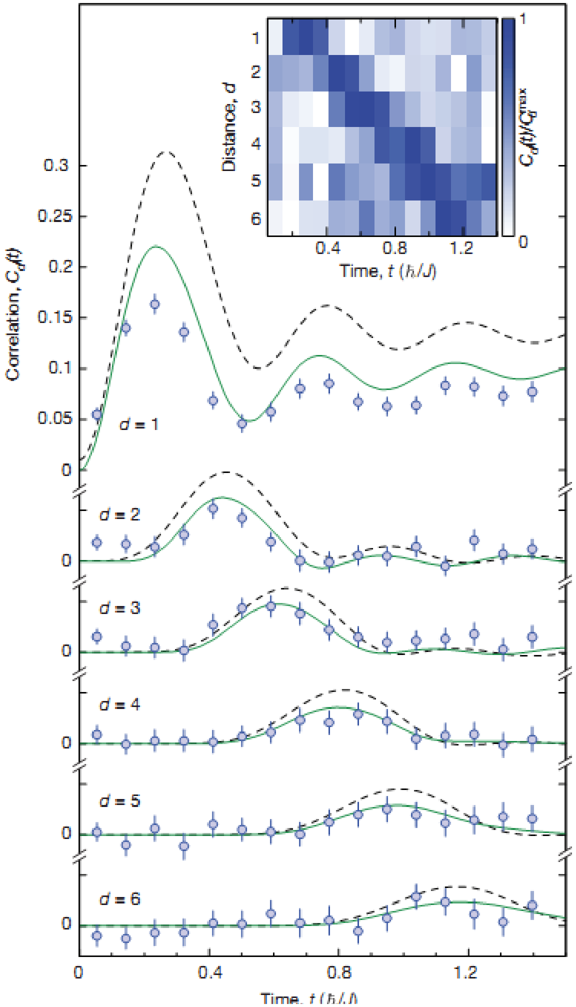

$$C_d(t) = \langle \hat{s}_j(t)\hat{s}_{j+d}(t)\rangle - \langle \hat{s}_j(t)\rangle\langle \hat{s}_{j+d}(t)\rangle$$

Nature (2012),Gross, Bloch… optical lattice

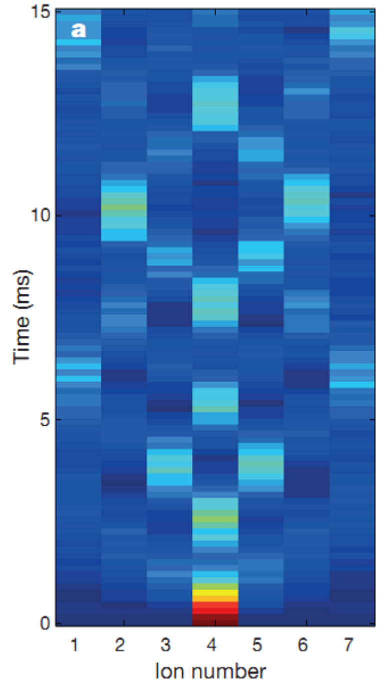

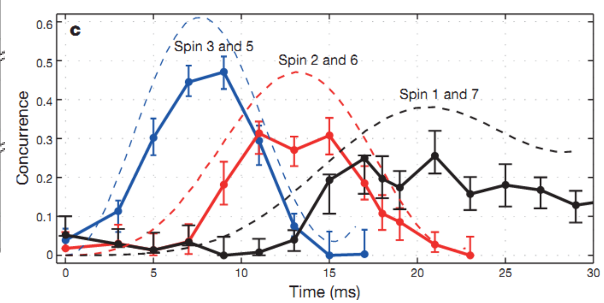

Nature (2014),Blatt, Roos… trapped ions

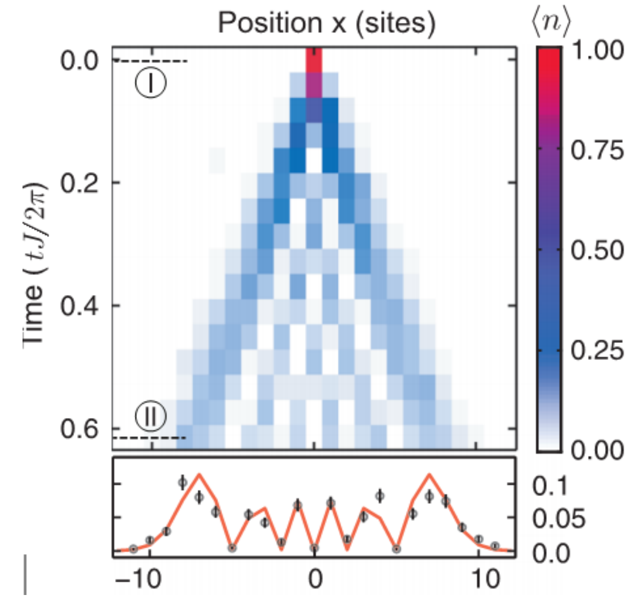

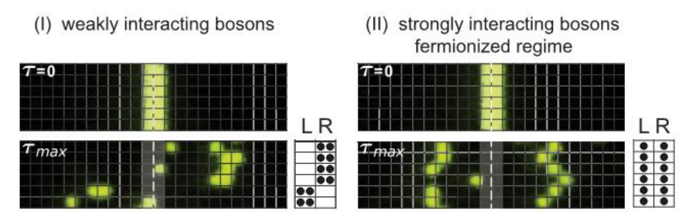

Science (2015), Greiner, …optical lattice

Entanglement propagation in a 12-qubit processor

归入量子态演化

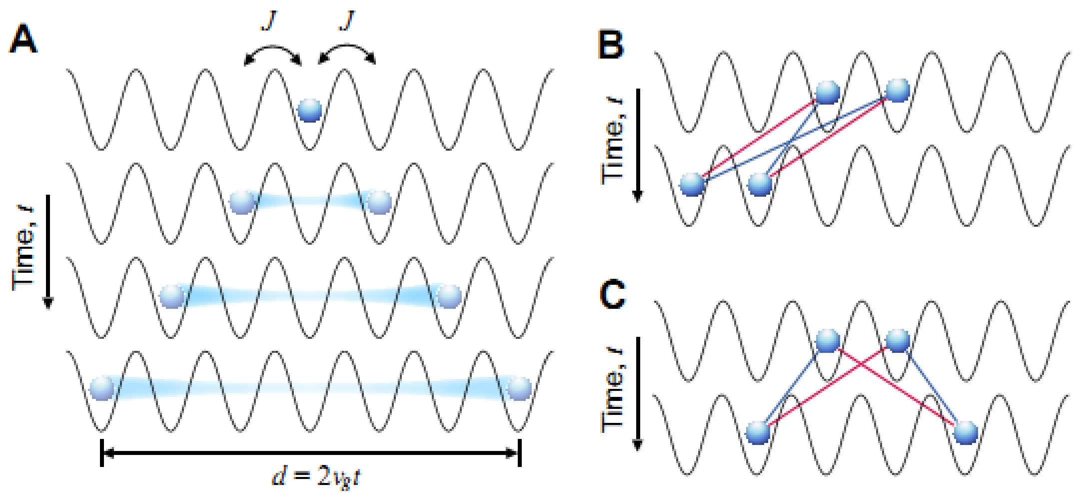

$$H = J\sum_{j=1}^{N-1}(\hat{a}_j^\dagger \hat{a}_{j+1} + \mathrm{h.c.}) + \frac{U}{2}\sum_{j=1}^{N}\hat{n}_j(\hat{n}_j - 1) + \sum_{j=1}^{N} h_j \hat{n}_j$$

Science REPORTS

Cite as: Z. Yan *et al.*, *Science*
10.1126/science.aaw1611 (2019).

Strongly correlated quantum walks with a 12-qubit superconducting processor

Zhiguang Yan[1,2*], Yu-Ran Zhang[3,4,5*], Ming Gong[1,2*], Yulin Wu[1,2], Yarui Zheng[1,2], Shaowei Li[1,2], Can Wang[1,2], Futian Liang[1,2], Jin Lin[1,2], Yu Xu[1,2], Cheng Guo[1,2], Lihua Sun[1,2], Cheng-Zhi Peng[1,2], Keyu Xia[6,7,4], Hui Deng[1,2], Hao Rong[1,2], J. Q. You[8,3], Franco Nori[4,9], Heng Fan[5,10†], Xiaobo Zhu[1,2†], Jian-Wei Pan[1,2]

Entanglement propagation in a 12-qubit processor

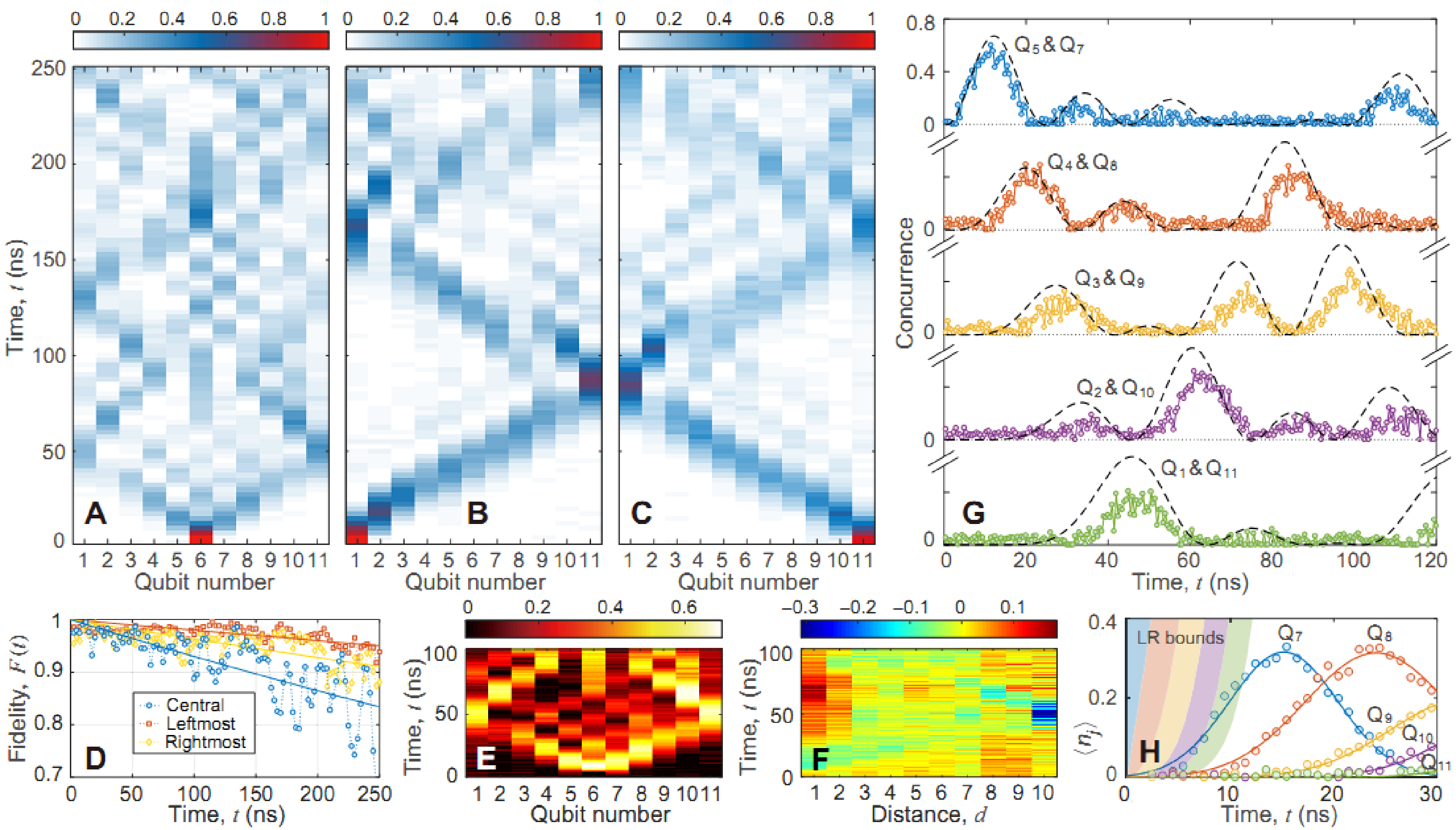

Science REPORTS

Cite as: Z. Yan *et al.*, *Science* 10.1126/science.aaw1611 (2019).

Strongly correlated quantum walks with a 12-qubit superconducting processor

Zhiguang Yan[1,2*], Yu-Ran Zhang[3,4,5*], Ming Gong[1,2*], Yulin Wu[1,2], Yarui Zheng[1,2], Shaowei Li[1,2], Can Wang[1,2], Futian Liang[1,2], Jin Lin[1,2], Yu Xu[1,2], Cheng Guo[1,2], Lihua Sun[1,2], Cheng-Zhi Peng[1,2], Keyu Xia[6,7,4], Hui Deng[1,2], Hao Rong[1,2], J. Q. You[8,3], Franco Nori[4,9], Heng Fan[5,10]†, Xiaobo Zhu[1,2]†, Jian-Wei Pan[1,2]

Entanglement propagation in a 12-qubit processor

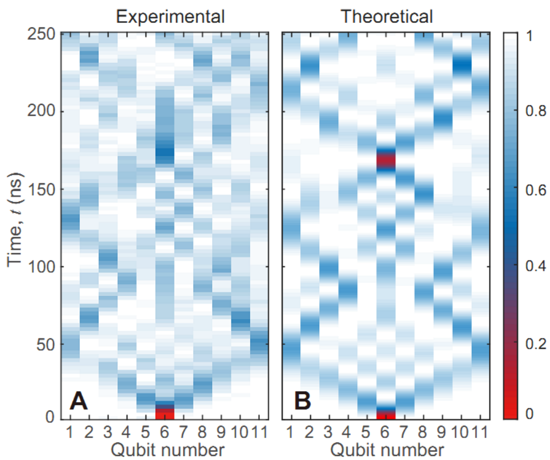

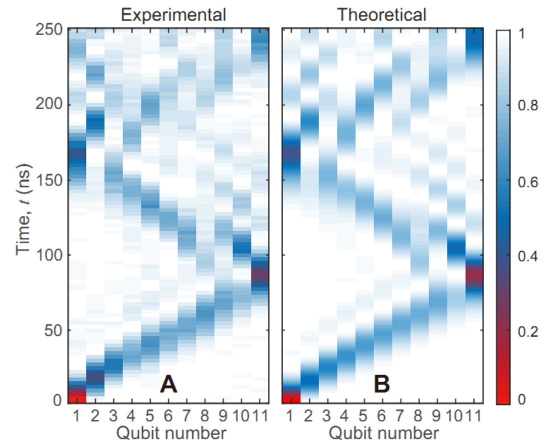

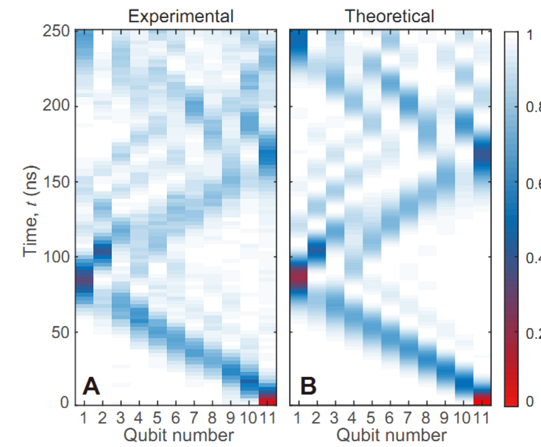

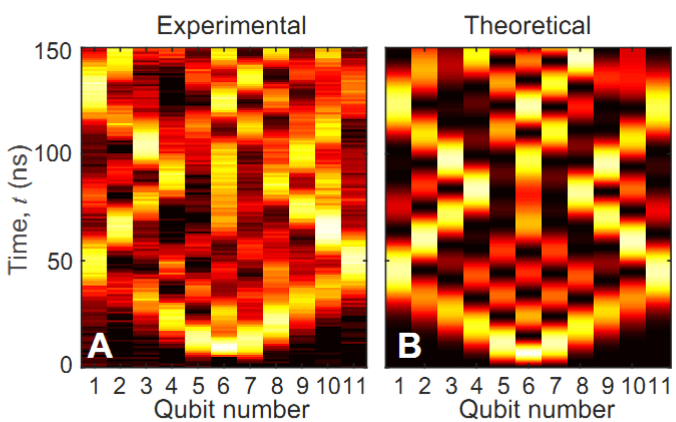

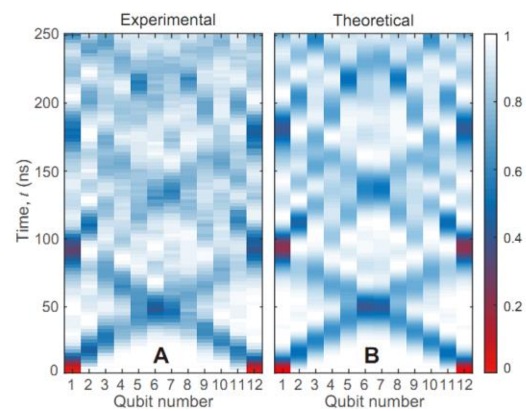

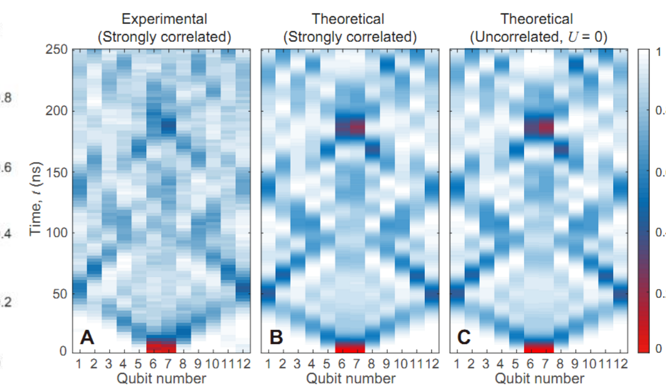

Comparison between theory and experiments

Science 364, 753 (2019)

Entanglement propagation in a 12-qubit processor

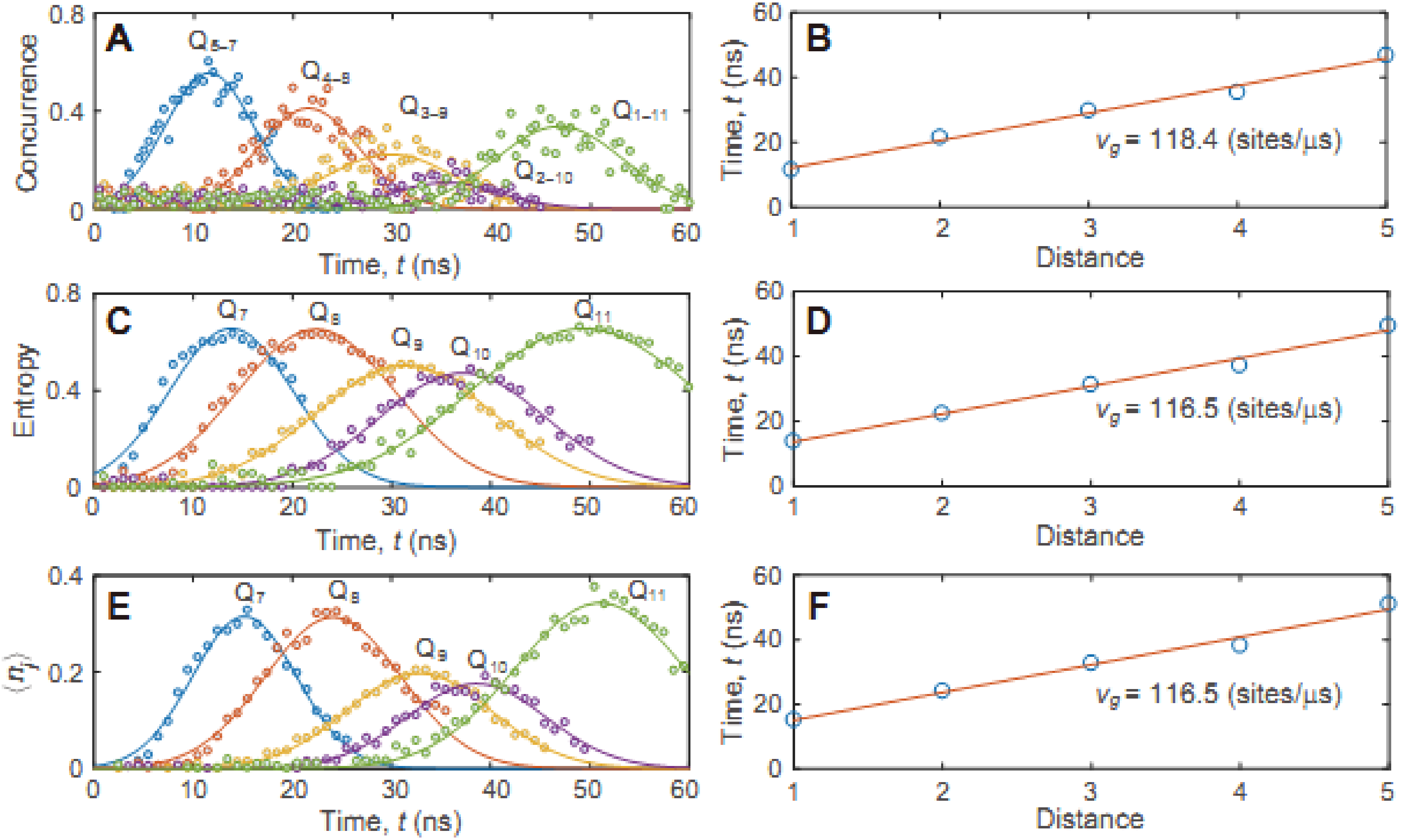

Lieb-Robinson bounds

Entanglement propagation in a 12-qubit processor

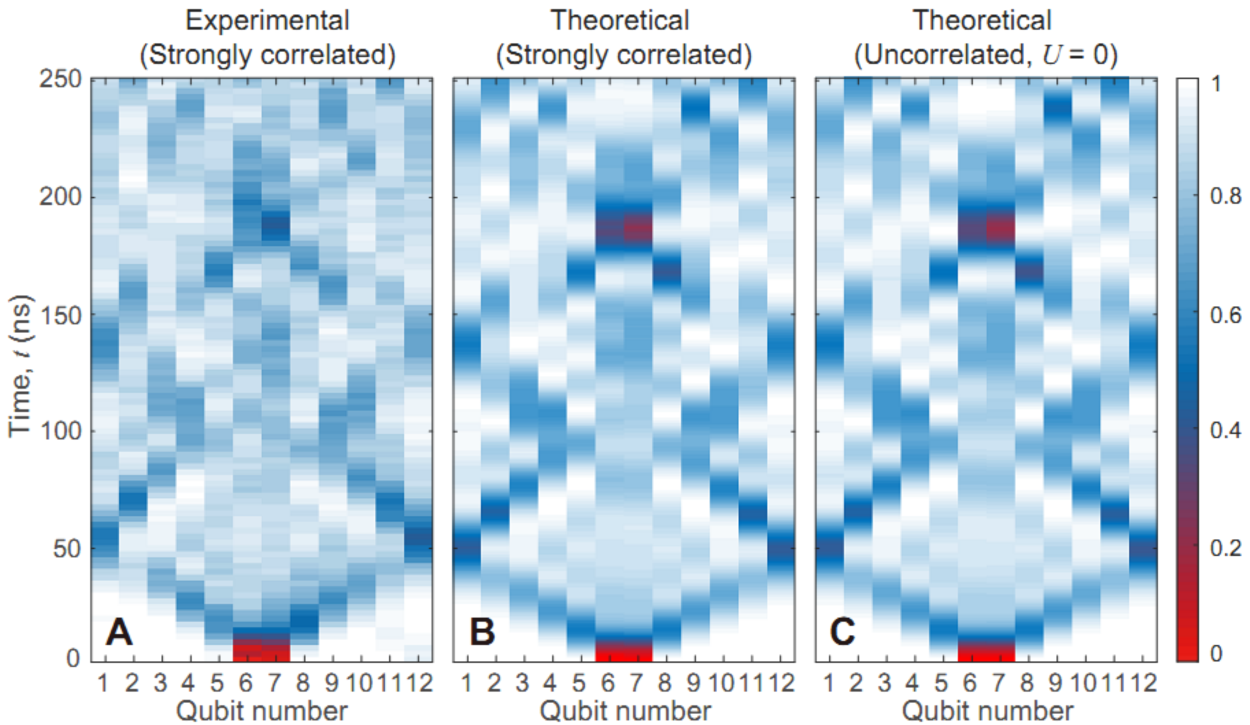

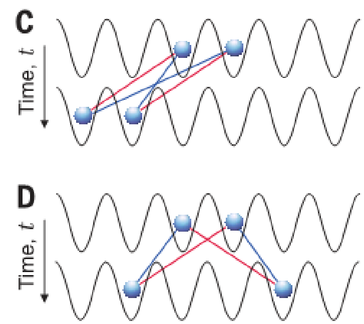

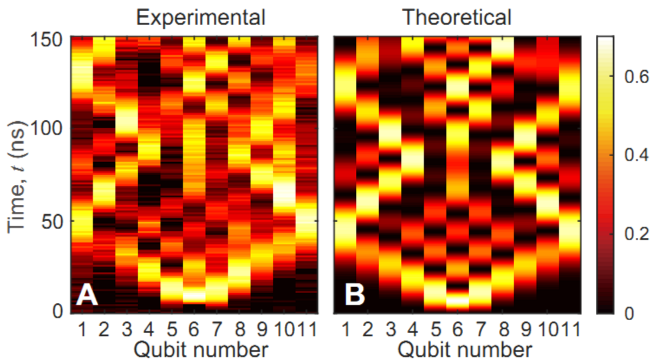

Two-particle QWs show similar density distributions

Science 364, 753 (2019)

Entanglement propagation in a 12-qubit processor

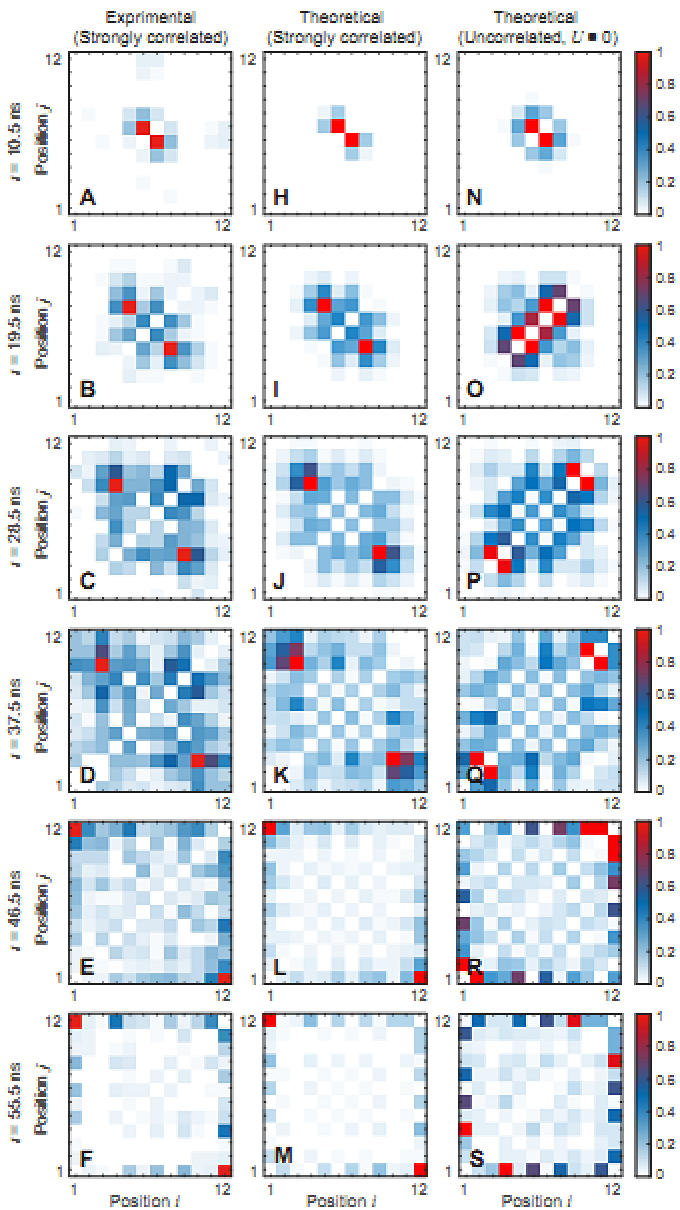

$$\Gamma_{ij} = \langle \hat{a}_i^\dagger \hat{a}_j^\dagger \hat{a}_i \hat{a}_j \rangle$$

Corresponding there are two particles at sites (i,j)

Strong on-site interaction (theoretical and experimental), without on-site interaction

Science 364, 753 (2019)

Entanglement propagation in a 12-qubit processor

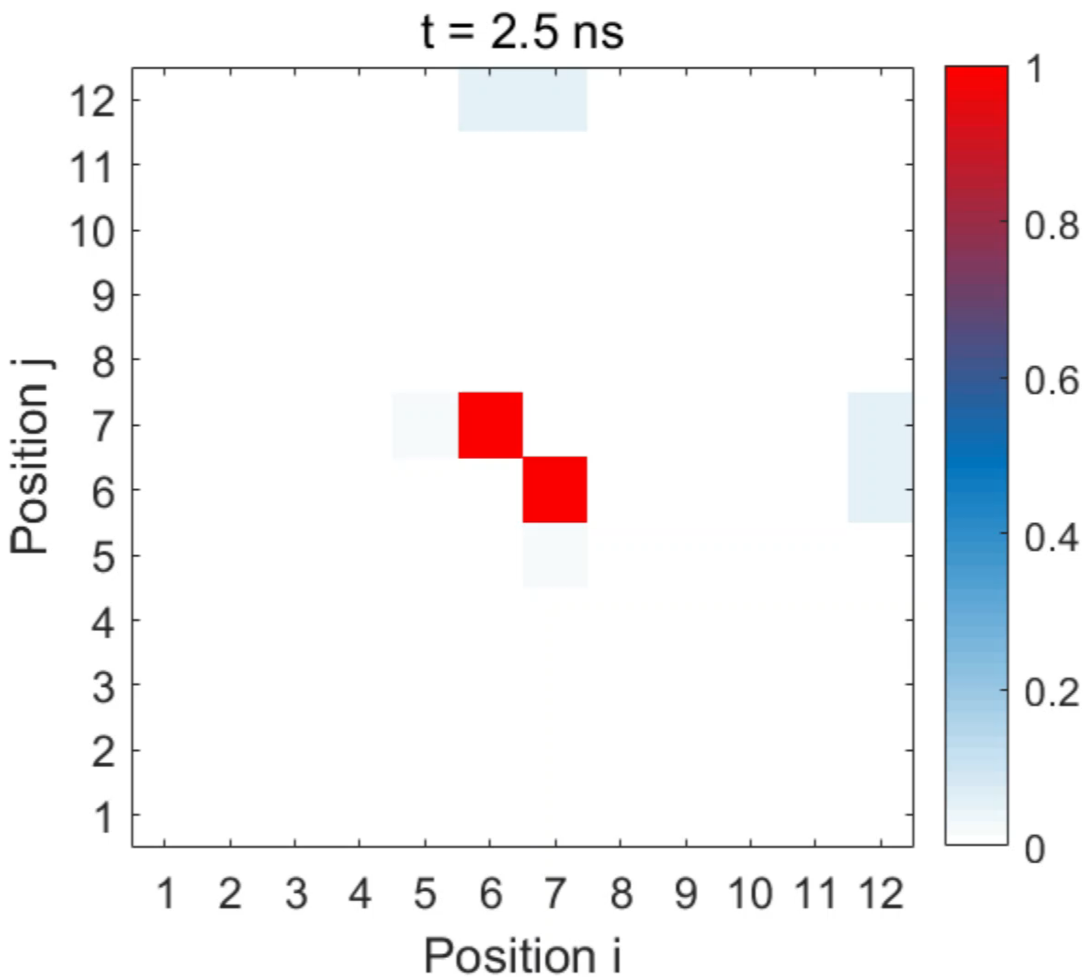

$$\Gamma_{ij} = \langle \hat{a}_i^{\dagger} \hat{a}_j^{\dagger} \hat{a}_i \hat{a}_j \rangle,$$

Simulation of dynamical quantum phase transition

$$H_{\text{Ising}} = -\sum_{i=1}^{N}\left(\sigma_i^x\sigma_{i+1}^x + g\sigma_i^z\right) \qquad H = \sum_k \Psi_k^\dagger h(k)\Psi_k$$

$$h(k) = d_0(k) + \mathbf{d}(k)\cdot\boldsymbol{\sigma},$$

$$\rho_i(k) = |\phi_i(k)\rangle\langle\phi_i(k)| = \frac{1}{2}\left[1 - \hat{\mathbf{d}}_i(k)\cdot\boldsymbol{\sigma}\right]$$

$$\rho(k,t) = |\phi(k,t)\rangle\langle\phi(k,t)| = \frac{1}{2}\left[1 - \hat{\mathbf{d}}(k,t)\cdot\boldsymbol{\sigma}\right].$$

$$\hat{\mathbf{d}}(k,t)\cdot\boldsymbol{\sigma} = e^{-it\mathbf{d}_f(k)\cdot\boldsymbol{\sigma}}\left(\hat{\mathbf{d}}_i(k)\cdot\boldsymbol{\sigma}\right)e^{it\mathbf{d}_f(k)\cdot\boldsymbol{\sigma}}$$

$$f(t) = -\frac{1}{N}\sum_k \log|\langle\phi_i(k)|e^{-ith_f(k)}|\phi_i(k)\rangle|^2.$$

Xue-Yi Guo, Chao Yang,…Shu Chen, Dongning Zheng, Heng Fan, Phys. Rev. Applied 11, 044080 (2019).

Simulation of dynamical quantum phase transition

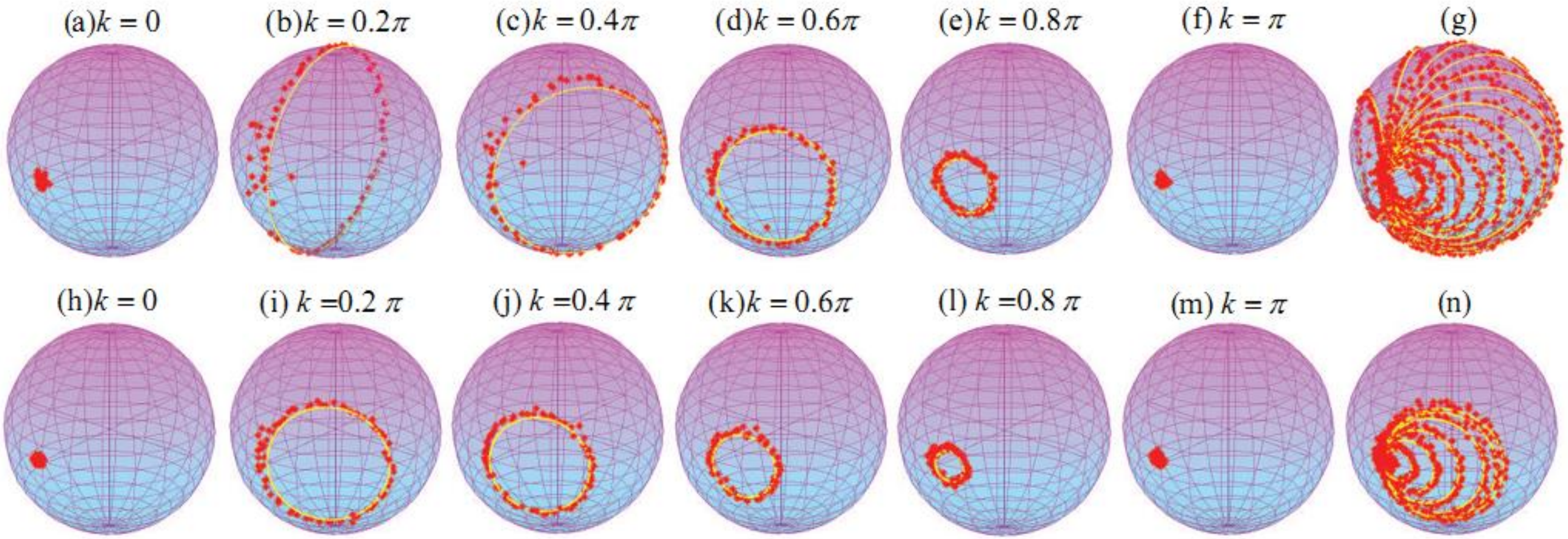

Here $g_i = 0.2$ is fixed, cases with $g_f = 1.5$ are presented in (a)-(g) in upper panel, cases of $g_f = 0.5$

Xue-Yi Guo, Chao Yang,…Shu Chen, Dongning Zheng, Heng Fan, Phys. Rev. Applied 11, 044080 (2019).

Simulation of quantum dynamical phase transition

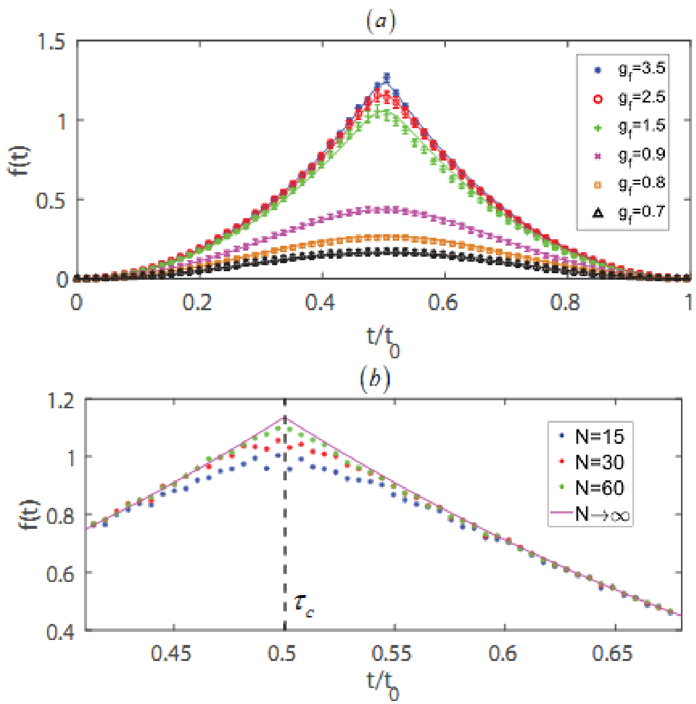

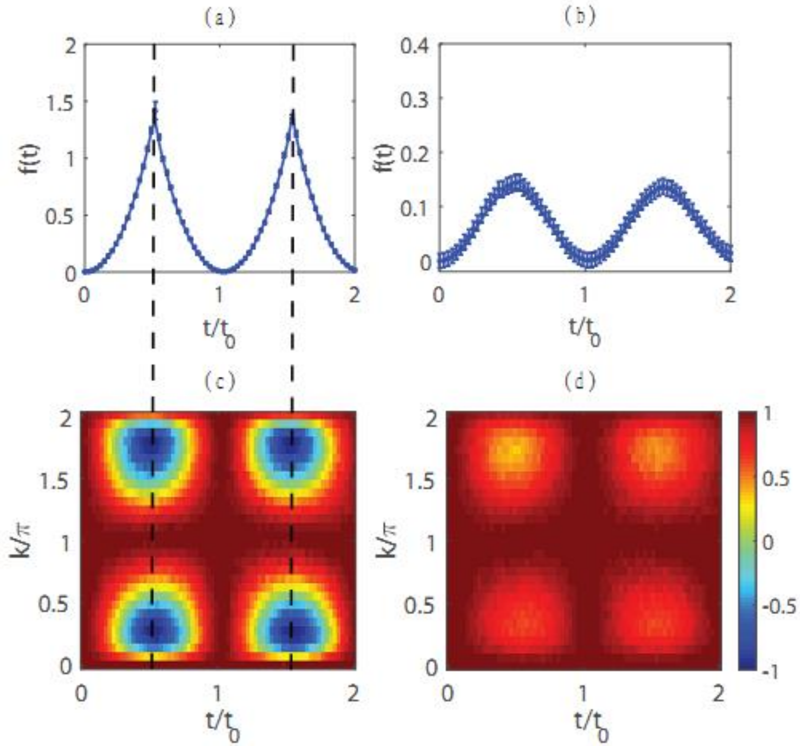

$$\langle \hat{\mathbf{d}}(\bar{k}, t)\rangle = \langle \phi(k,t)|\hat{\mathbf{d}}_i|\phi(k,t)\rangle.$$

PHYSICAL REVIEW APPLIED **11,** 044080 (2019)

Observation of a Dynamical Quantum Phase Transition by a Superconducting Qubit Simulation

Xue-Yi Guo,[1,2] Chao Yang,[1,2] Yu Zeng,[1,2] Yi Peng,[1,2] He-Kang Li,[1,2] Hui Deng,[3] Yi-Rong Jin,[1,4] Shu Chen,[1,2,*] Dongning Zheng,[1,2,4,5,†] and Heng Fan[1,2,4,5,‡]

Criterion of genuine multipartite entanglement

Table 1
Results on local decompositions of different entanglement witnesses for different states.

# of qubits	state	witness	maximal p_{noise}	local measurements	references	remarks
3	$\lvert GHZ_3\rangle$	$\frac{1}{2}\mathbb{1} - \lvert GHZ_3\rangle\langle GHZ_3\rvert$	4/7	4 (optimal)	[387]	a
3	$\lvert W_3\rangle$	$\frac{2}{3}\mathbb{1} - \lvert W_3\rangle\langle W_3\rvert$	8/21	5 (optimal)	[387]	b
4	$\lvert CL_4\rangle$	$\frac{1}{2}\mathbb{1} - \lvert CL_4\rangle\langle CL_4\rvert$	8/15	9 (optimal)	[388, 391]	a
4	$\lvert\Psi_2\rangle$	$\frac{3}{4}\mathbb{1} - \lvert\Psi_2\rangle\langle\Psi_2\rvert$	4/15	15	[145, 390]	c
4	$\lvert D_{2,4}\rangle$	$\frac{2}{3}\mathbb{1} - \lvert D_{2,4}\rangle\langle D_{2,4}\rvert$	16/45	21	[213]	d
N	$\lvert GHZ_N\rangle$	$\frac{1}{2}\mathbb{1} - \lvert GHZ_N\rangle\langle GHZ_N\rvert$	$1/2 \cdot [1/(1-1/2^N)]$	$N+1$	[390]	a
N	$\lvert W_N\rangle$	$\frac{N-1}{N}\mathbb{1} - \lvert W_N\rangle\langle W_N\rvert$	$1/N \cdot [1/(1-1/2^N)]$	$2N-1$	[8, 390]	b
N	$\lvert G_N\rangle$	$\frac{1}{2}\mathbb{1} - \lvert G_N\rangle\langle G_N\rvert$	$1/2 \cdot [1/(1-1/2^N)]$	depends on the graph	[264]	a
N	$\lvert D_{\frac{N}{2},N}\rangle$	$\frac{N}{2N-2}\mathbb{1} - \lvert D_{\frac{N}{2},N}\rangle\langle D_{\frac{N}{2},N}\rvert$	$1/2 \cdot (N-2)/[(N-1)(1-1/2^N)]$	not known	[213]	

[a] Witnesses that tolerate less noise but require less settings exist. See Section 6.6.1.
[b] Witnesses that tolerate more noise with the same measurements exist. See Sections 6.8.2 and 8.2.
[c] Witnesses that tolerate more noise and require less settings exist [190, 390].
[d] For witnesses that tolerate less noise with less settings see Section 8.2, for witnesses which tolerate more noise see Ref. [190].

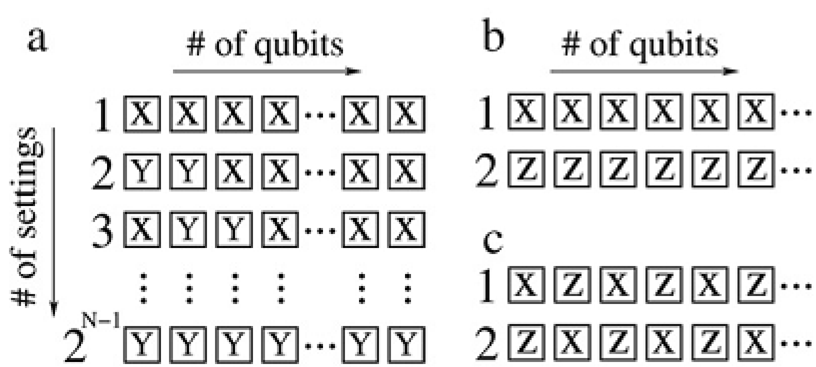

Physics Reports (2009)

Multicomponent Schrodinger cat state-GHZ

$$\frac{H_2}{\hbar} = \sum_{\{j,k\}\in N} \frac{g_j g_k}{\Delta}\left(\sigma_j^+\sigma_k^- + \sigma_j^-\sigma_k^+\right) + \sum_{j=1}^{N} \frac{g_j^2}{\Delta}|1_j\rangle\langle 1_j| + \sum_{j=1}^{N} \lambda_{j,j+1}^{c}\left(\sigma_j^+\sigma_{j+1}^- + \sigma_j^-\sigma_{j+1}^+\right)$$

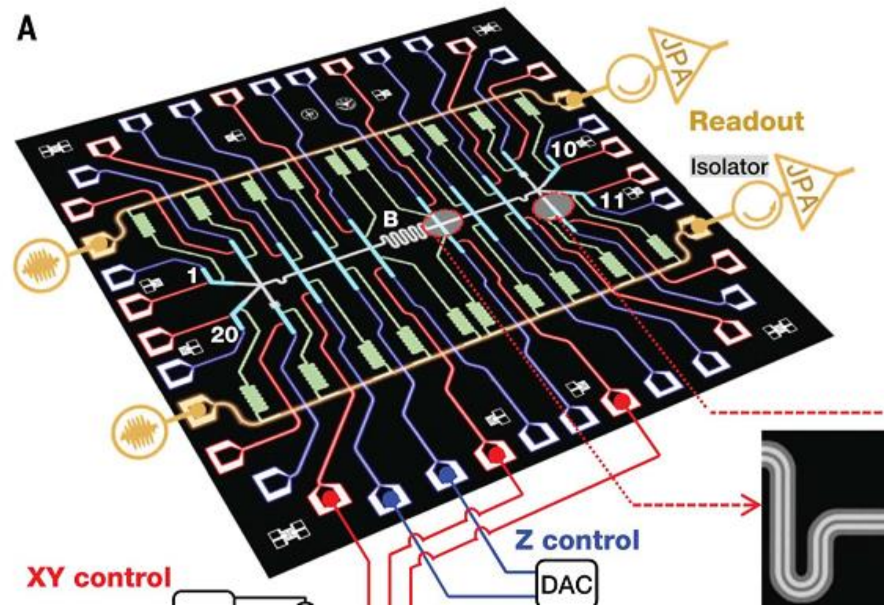

RESEARCH

QUANTUM PHYSICS

Generation of multicomponent atomic Schrödinger cat states of up to 20 qubits

Chao Song[1]*, Kai Xu[2,3]*, Hekang Li[2]*, Yu-Ran Zhang[2,4], Xu Zhang[1], Wuxin Liu[1], Qiujiang Guo[1], Zhen Wang[1], Wenhui Ren[1], Jie Hao[5], Hui Feng[5], Heng Fan[2,3]†, Dongning Zheng[2,3]†, Da-Wei Wang[1,3], H. Wang[1,6]†, Shi-Yao Zhu[1,6]

Science 365, 574 (2019).

Multicomponent Schrodinger cat state-GHZ

$$H_2/\hbar = \sum_{\{j,k\}\in N} \frac{g_j g_k}{\Delta}\left(\sigma_j^+\sigma_k^- + \sigma_j^-\sigma_k^+\right) + \sum_{j=1}^{N}\frac{g_j^2}{\Delta}\left|1_j\right\rangle\left\langle 1_j\right| + \sum_{j=1}^{N}\lambda_{j,j+1}^{c}\left(\sigma_j^+\sigma_{j+1}^- + \sigma_j^-\sigma_{j+1}^+\right), \quad (2)$$

$$S^+ = \sum_j \sigma_j^+,\ S^- = \sum_j \sigma_j^-, \qquad S_z = \sum_j \sigma_{z,j}.$$

$$\sum \lambda\left(\sigma_j^+\sigma_k^- + \sigma_j^-\sigma_k^+\right) \Rightarrow \lambda S^+ S^- \rightarrow -\lambda S_z^2$$

$$\left(|0\rangle - i\,|1\rangle\right)/\sqrt{2} \qquad \left(|00\ldots0\rangle + e^{i\varphi}|11\ldots1\rangle\right)/\sqrt{2},$$

Science 365, 574 (2019).

Observation of multi-component atomic Schrödinger cat states of up to 20 qubits

Chao Song[1,*] Kai Xu[2,4,*] Hekang Li[2,*] Yuran Zhang[2,5], Xu Zhang[1], Wuxin Liu[1], Qiujiang Guo[1], Zhen Wang[1], Wenhui Ren[1], Jie Hao[3], Hui Feng[3], Heng Fan[2,4,†] Dongning Zheng[2,4,‡] Dawei Wang[1,4], H. Wang[1,6,§] and Shiyao Zhu[1,6]

Multicomponent Schrodinger cat state-GHZ

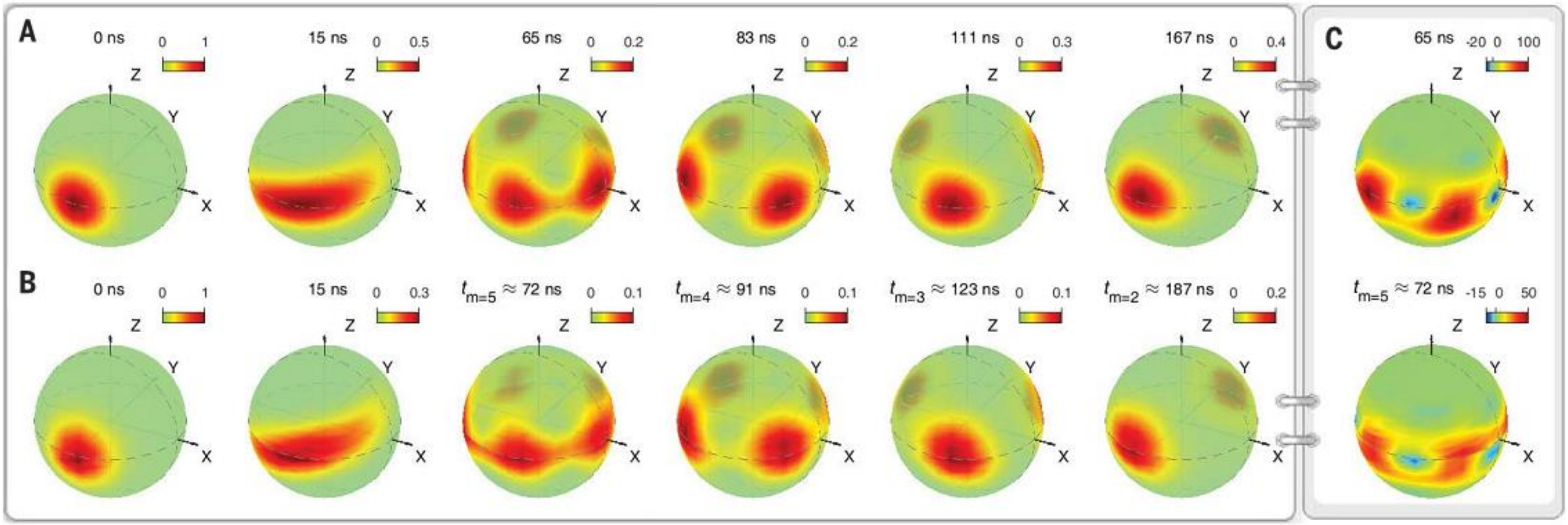

RESEARCH

QUANTUM PHYSICS

Generation of multicomponent atomic Schrödinger cat states of up to 20 qubits

Chao Song[1]*, Kai Xu[2,3]*, Hekang Li[2]*, Yu-Ran Zhang[2,4], Xu Zhang[1], Wuxin Liu[1], Qiujiang Guo[1], Zhen Wang[1], Wenhui Ren[1], Jie Hao[5], Hui Feng[5], Heng Fan[2,3]†, Dongning Zheng[2,3]†, Da-Wei Wang[1,3], H. Wang[1,6]†, Shi-Yao Zhu[1,6]

Science 365, 574 (2019).

Multicomponent Schrodinger cat state-GHZ

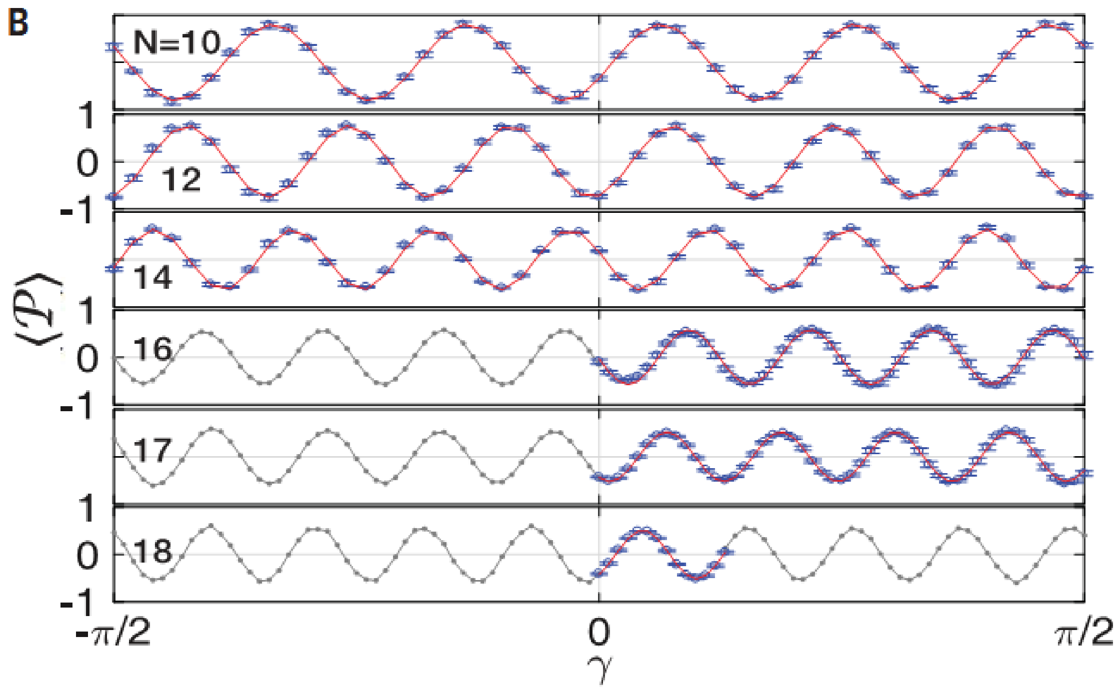

$[|00...0\rangle + \exp(i\varphi)|11...1\rangle]/\sqrt{2},$

$\langle\mathcal{P}(\gamma)\rangle = 2|\rho_{00...0,11...1}|\cos(N\gamma+\varphi)$

$$F = (P + C)/2$$

$$C = |\rho_{0...0,1...1}| + |\rho_{1...1,0...0}|$$

in $|1\rangle$. The amplitude of the oscillation patterns of $\langle\mathcal{P}(\gamma)\rangle$ gives $|\rho_{00...0,11...1}|$ (Fig. 2B). Using values of $\rho_{00...0}$, $\rho_{11...1}$, and $|\rho_{00...0,11...1}|$, N-qubit GHZ state fidelities $\mathcal{F}$ are calculated as 0.817 ± 0.009 ($N = 10$), 0.775 ± 0.011 ($N = 12$), 0.655 ± 0.009 ($N = 14$), 0.579 ± 0.007 ($N = 16$), 0.549 ± 0.006 ($N = 17$), and 0.525 ± 0.005 ($N = 18$), all confirming genuine multipartite entanglement with $\mathcal{F} > 0.5$ (24).

保真度50%对多比特系统实际正确率很高

Science 365, 574 (2019).

IBM Graph state (arbitrary bipartition)

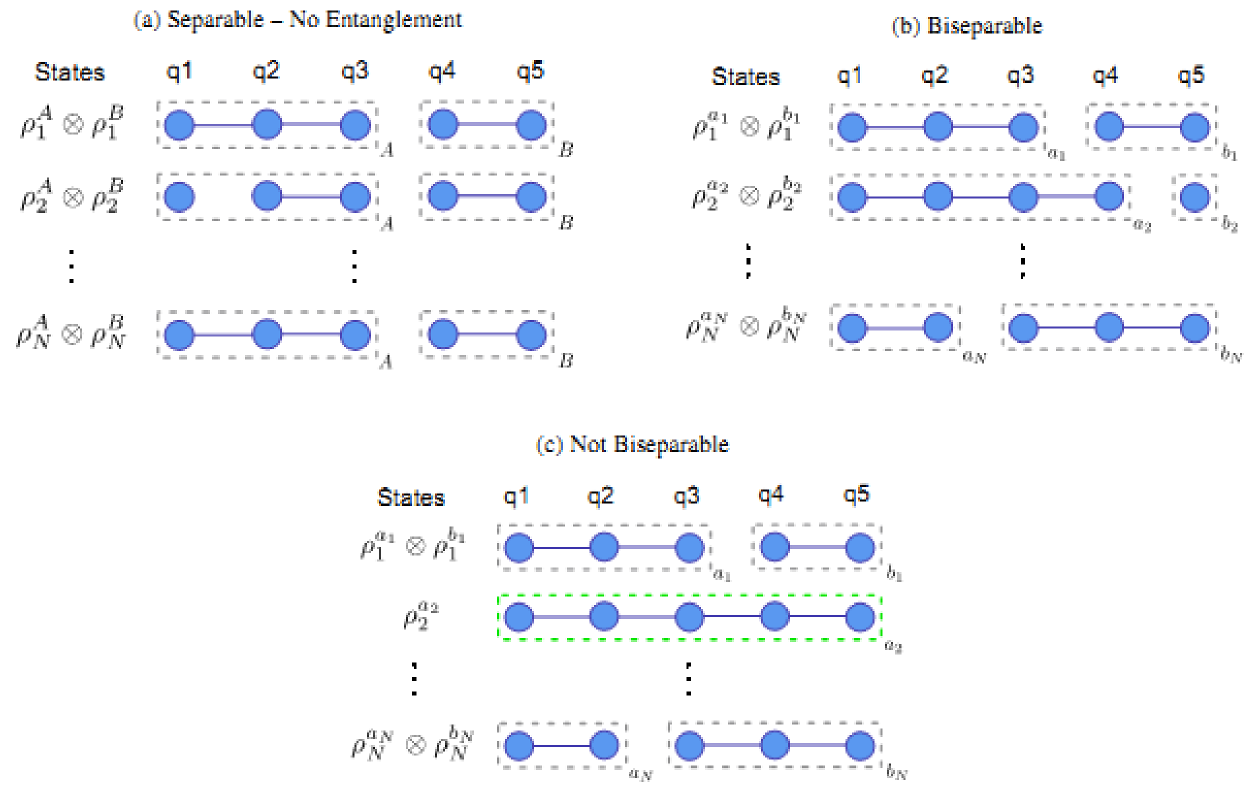

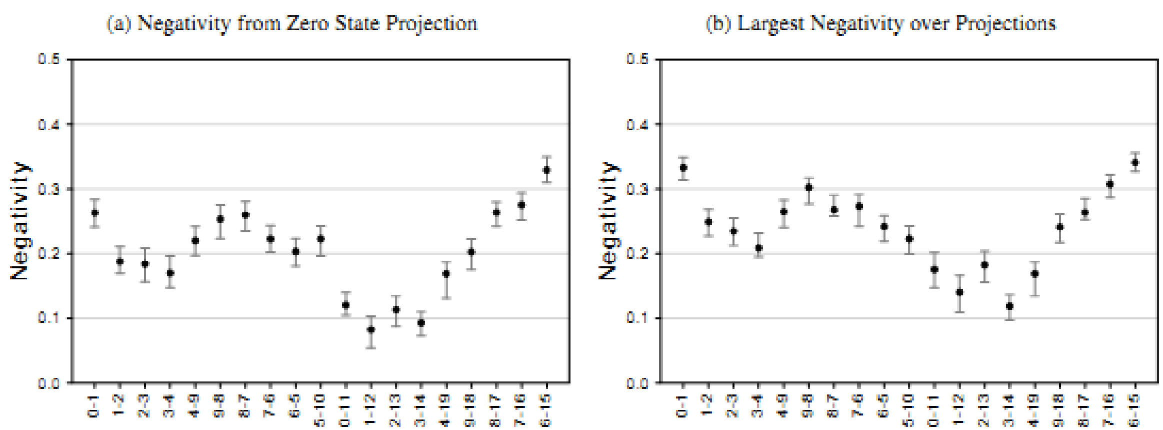

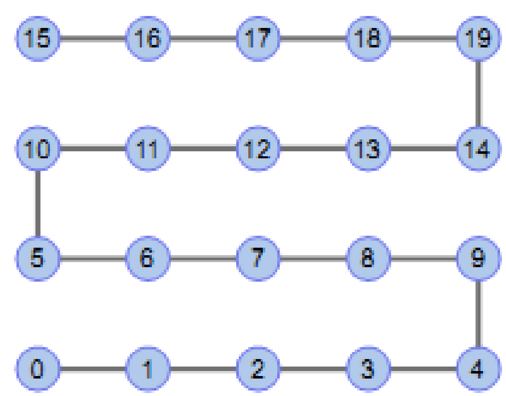

4

GHZ state preparation

Three independent works about GHZ state preparation

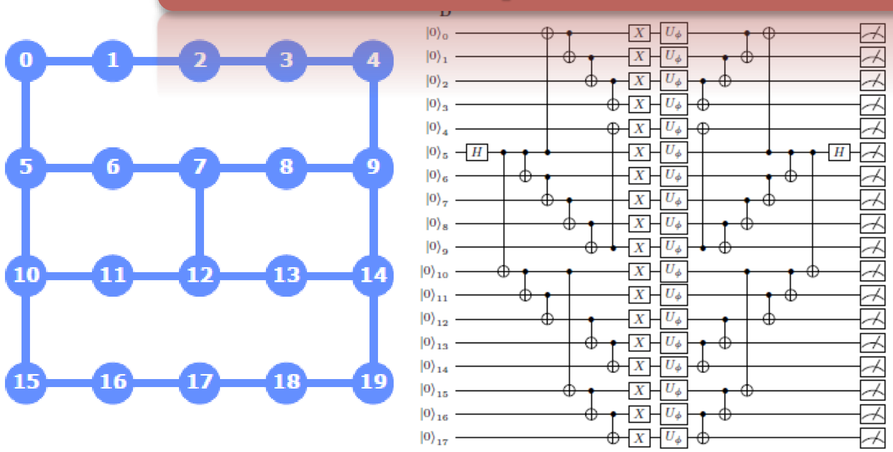

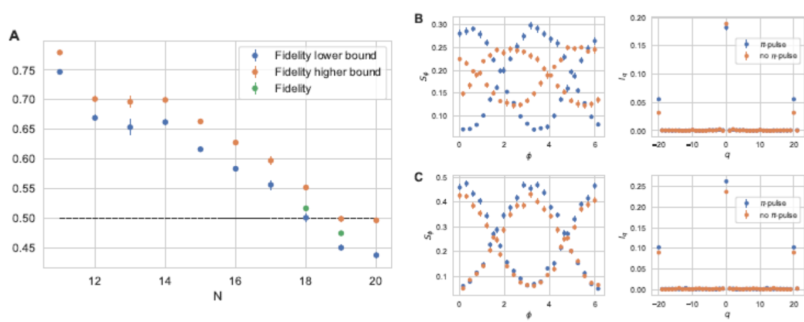

ment. For $N = 18$ the lower bound is 0.5006 ± 0.0067, in this case we measure $P_{000..00}$ and $P_{111..11}$ for the GHZ state in addition to MQC amplitudes to obtain the state fidelity of $F = 0.5165 \pm 0.0036$, confirming that the 18-

IBM group 18 superconducting qubits GHZ state, arXiv:1905.05720.

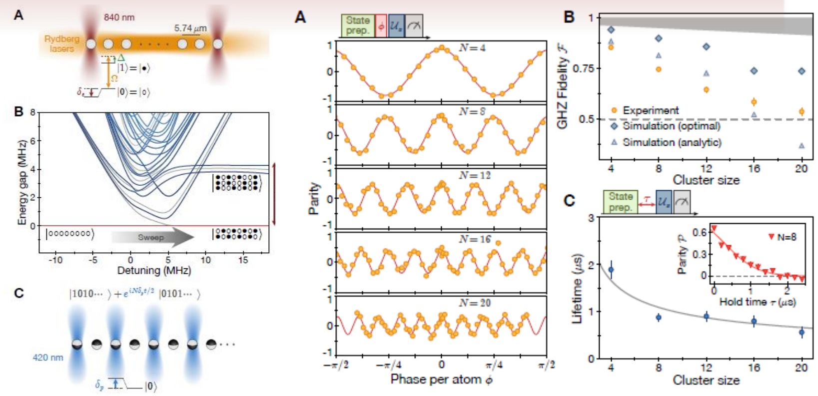

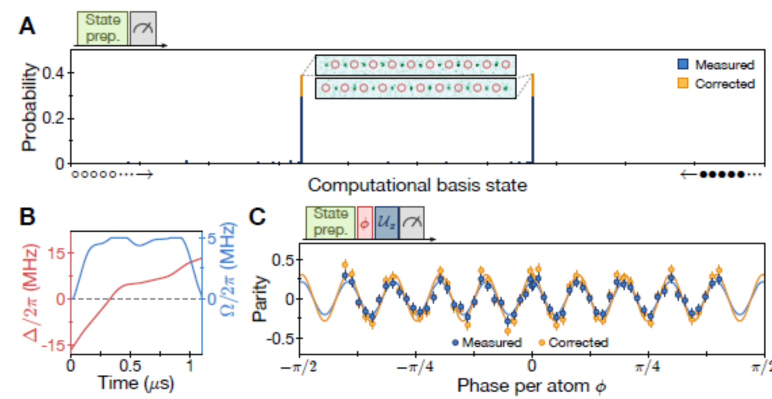

20-atom GHZ fidelity of $\mathcal{F} \geq 0.542(18)$

Harvard Lukin group 20-qubit GHZ arXiv:1905.05721.
Science 365, 570 (2019).

5 谷歌利用超导量子比特器件展示量子优势

计算任务：对于一个由量子线路定义的叠加态，找出百万个振幅较大的比特串

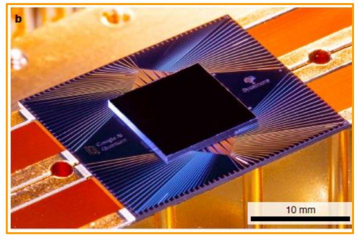

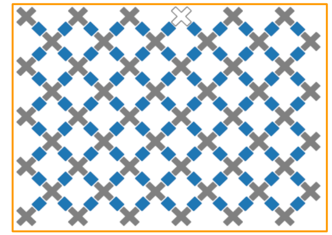

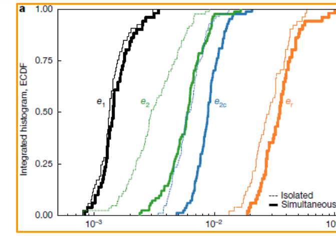

器件　　量子比特二维格点布局　　逻辑门保真度

量子线路作用于53个量子比特，一层单比特门一层双比特门共2*20层构成

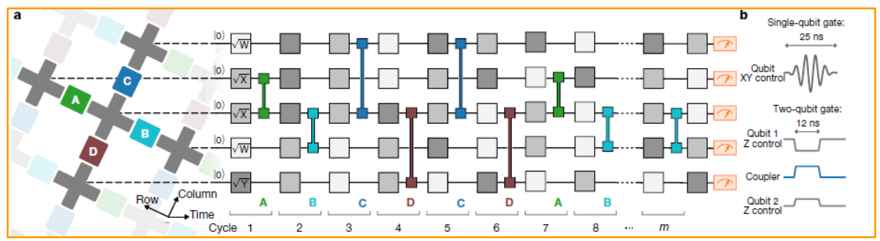

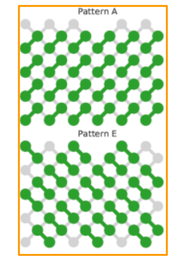

量子线路构成　　双比特门模式

谷歌宣称：最复杂的线路，实验可以实现准确率从随机选取的50%上升为50.1%。(b从1变为1.002)

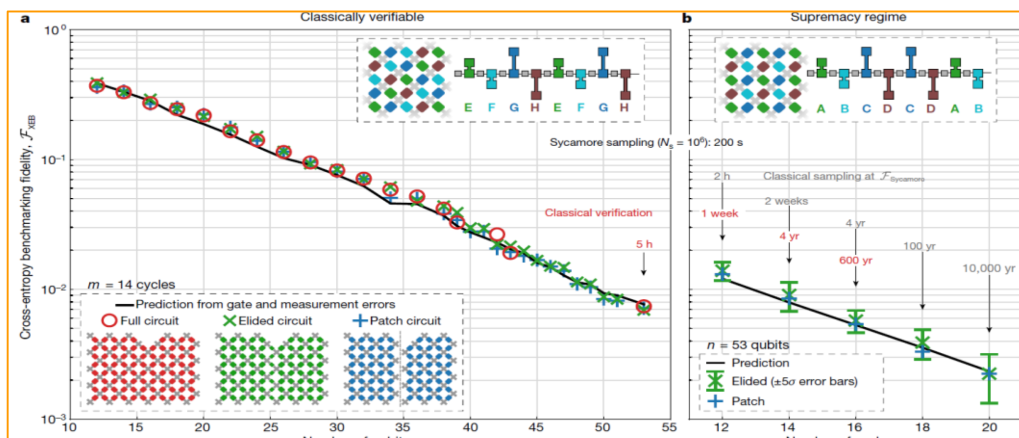

量子优势：随机量子线路采样方案

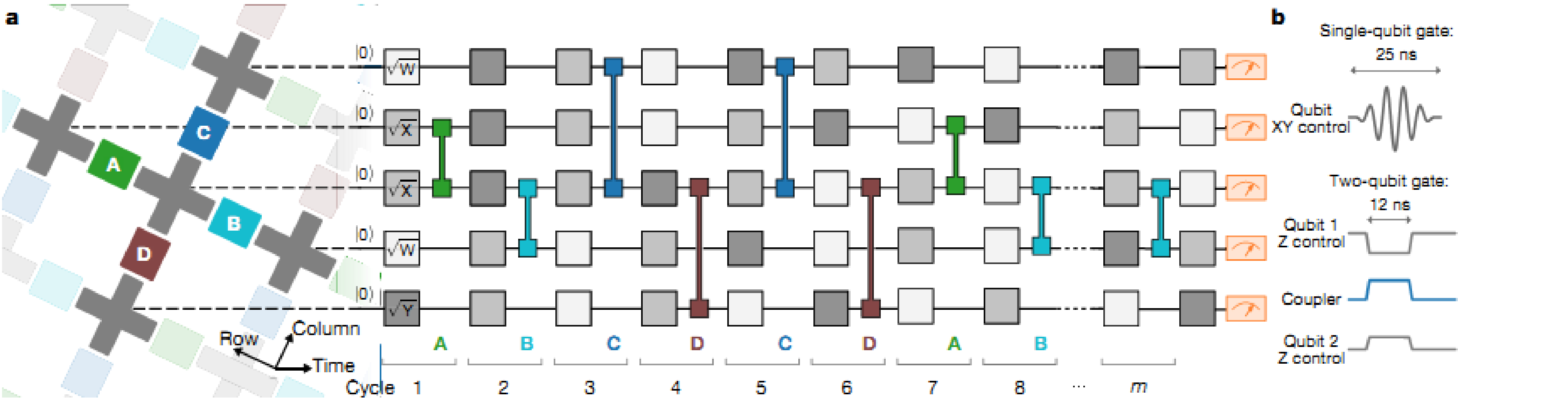

5比特，深度m的随机量子线路

$$X^{1/2} \equiv R_X(\pi/2) = \frac{1}{\sqrt{2}}\begin{bmatrix} 1 & -i \\ -i & 1 \end{bmatrix},$$

$$Y^{1/2} \equiv R_Y(\pi/2) = \frac{1}{\sqrt{2}}\begin{bmatrix} 1 & -1 \\ 1 & 1 \end{bmatrix},$$

$$W^{1/2} \equiv R_{X+Y}(\pi/2) = \frac{1}{\sqrt{2}}\begin{bmatrix} 1 & -\sqrt{i} \\ \sqrt{-i} & 1 \end{bmatrix}$$

$$\mathrm{fSim}(\theta,\phi) = e^{-i\theta(X\otimes X+Y\otimes Y)/2}\, e^{-i\phi(I-Z)\otimes(I-Z)/4}$$

$$\mathrm{fSim}(\theta,\phi) = \begin{bmatrix} 1 & 0 & 0 & 0 \\ 0 & \cos(\theta) & -i\sin(\theta) & 0 \\ 0 & -i\sin(\theta) & \cos(\theta) & 0 \\ 0 & 0 & 0 & e^{-i\phi} \end{bmatrix}$$

$$\theta \approx \pi/2 \text{ and } \phi \approx \pi/6$$

iSWAP and CZ

single-qubit gates chosen randomly from $\{\sqrt{X}, \sqrt{Y}, \sqrt{W}\}$ on all qubits

5 Quantum Supremacy

执行随机量子线路操作U后，我们会得到一个维度为2^{53}维希尔伯特空间的量子态$|\Psi\rangle = \mathrm{U}|\vec{0}\rangle$，同时对53个量子比特进行测量，得到一个53位的比特串，$x_j \in \{0,1\}^{53}$，即一次采样结果，对确定的一种线路重复测量百万次，即采样百万次，结果是百万个比特串$\{x_j\}_{j=1}^{k}$，k=10^6，使之满足不等式，

$$\frac{1}{k}\sum_{j=1}^{k}|\langle x_j|\mathrm{U}|\vec{0}\rangle|^2 \geq \frac{b}{2^{53}}, \qquad \mathrm{D}=2^{53}$$

对一个随机量子线路，几率幅处于$[p, p+dp]$的比特串占比为$\Pr(p)\,dp = De^{-Dp}dp$，即$\Pr(p)$是比特串密度（多少）按照其振幅p的分布函数，这个分布函数符合Porter-Thomas分布，几率幅处于$[p, p+dp]$的比特串总数为$\mathrm{N}(p)dp = D\Pr(p)\,dp = D^2e^{-Dp}dp$,

已知采样比特串的分布函数$f(p)$，需要求得$\{p(x_j)\}_{j=1}^{k}$的平均值，可以得到$\langle \mathrm{p}\rangle = \int_0^1 pf(p)dp = \int_0^1 p^2D^2e^{-Dp}dp \approx \frac{2}{D}$

理想情况100%正确b=2；噪音无穷大, 即随机选取b=1.
实验得到b=1.002, 即正确率从随机的50%上升为50.1%

7 问答

量子计算（态）的空间是指数增长

$$|\psi\rangle = \sum_{j_1 j_2 \dots j_N = 0}^{1} x_{j_1 j_2 \dots j_N} |j_1\rangle |j_2\rangle \dots |j_N\rangle$$

共有2^N**个参数** $x_{j_1 j_2 \dots j_N}$

量子计算即是对量子态进行操作，导致2^N**个参数变化，一个53个量子比特的操作带来**10^{16}**个数据的相应变化，用经典计算机是不可能完成的！**

所以，量子计算机是不可替代的，如果我们先不管它做的任务是有用还是无用

7 问答

量子模拟非常适合做动力学问题，比如哈密顿量含时，量子态在此哈密顿量作用下进行动力学演化。

量子态共含有2^N个参数，所以测量所有的参数值是不可能做到的！

量子计算最终结果的测量应该是对某些观测量的测量，不能涉及指数增长需求的测量方案，理想的选择是给出是和否的答案的测量。

量子模拟一般从初态出发，初态制备不能很难，但是任意直积态可以比较容易制备。所以量子模拟对于坐标变换一般是容易的。

7 问答：量子工程-科研应用

噪音预期在短期（10年）不可很小，所以现实的方案选择也许是优化选择，正确率上升，趋势判断等问题

量子计算机解决量子问题有优势！

超过50个量子比特，动力学，含时操控，没有好的经典方法，最终结果含有指数增长的信息（量子态），但是答案是经典的---

好的量子优势方案！

7 问答

量子优势时，量子计算机的任务不可能用经典计算机给出答案

如何知道量子计算给出的答案正确还是错误？

1. **可以采取趋势标定错误率的形式：简单情况标定噪音随比特数和时间的趋势，估计复杂情况的错误率**
2. **复杂计算错误率同一个简化的计算形式相差不大，类比得到估计值。**

Thank you

谢谢！